HELMHOLTZ | GEMEINSCHAFT
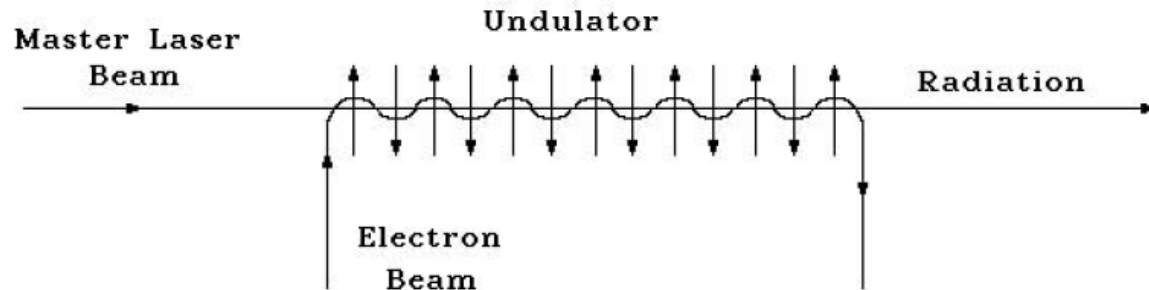
Coherence properties of the radiation from SASE FEL

M.V. Yurkov

DESY, Hamburg

I.   Start-up of the FEL process from shot noise: SASE FEL.
II. Longitudinal coherence (temporal and spectral properties). Statistics.
III. Transverse coherence.
IV. Higher harmonics.

# What we name as X-ray FEL, SASE FEL, etc.

- **FEL** stands for free electron laser.
- **FEL amplifier** stands for single-pass free electron laser amplifier.
- **X-ray FEL / XFEL** stands for x-ray free electron laser. This is FEL amplifier starting form the shot noise in the electron beam and operating in the x-ray wavelength range.
- **SASE FEL** stands for self-amplified spontaneous emission free electron laser. This quantum terminology does not reflect actual physics of the device, but is widely used. Physically SASE FEL means FEL amplifier starting from shot noise in the electron beam – device which forms separate class of vacuum tube electronics. Close relative of the FEL is travelling wave tube (TWT).
- Slang of the FEL community usually uses x-ray FEL, XFEL, and SASE FEL as synonyms.

Undulator

Output radiation

Electron beam
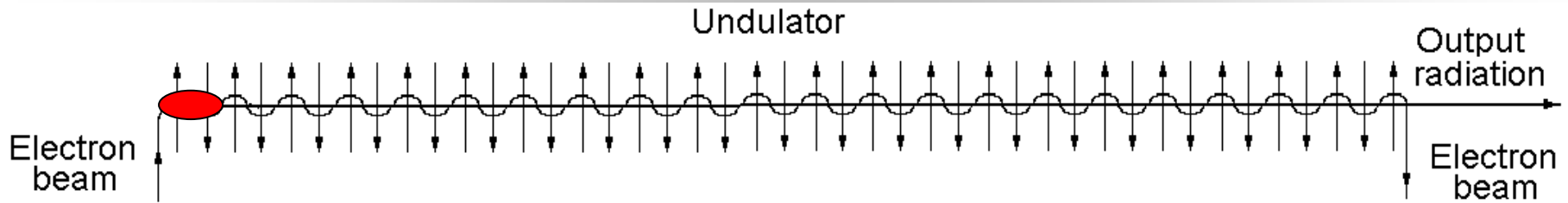
Electron beam

- A single-pass free electron laser starting from the shot noise in the electron beam looks to be similar to the well known undulator insertion device: in both cases radiation is produced during single pass of the electron beam through the undulator.

- Central wavelength is the same: $\lambda = (\lambda_{\mathrm{w}}/2\gamma^2)(1 + K^2)$.

- Principal difference relates to the detailes of the distribution of the particles in the beam: in the free electron laser, electron beam density is modulated by the period of resonance wavelength λ.

- Enhancement of the beam modulation in the free electron laser occurs due to the radiation-induced collective instability.

- Radiation power from modulated electron beam holds potential to exceed the power of incoherent radiation by a factor of number of electrons in the volume of coherence, $N_{\mathrm{c}} = N_\lambda \times N_{\mathrm{w}}$.

$P \propto \exp[2z/L_{\mathrm{g}}]$
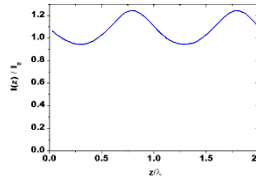
TTF FEL, 2001
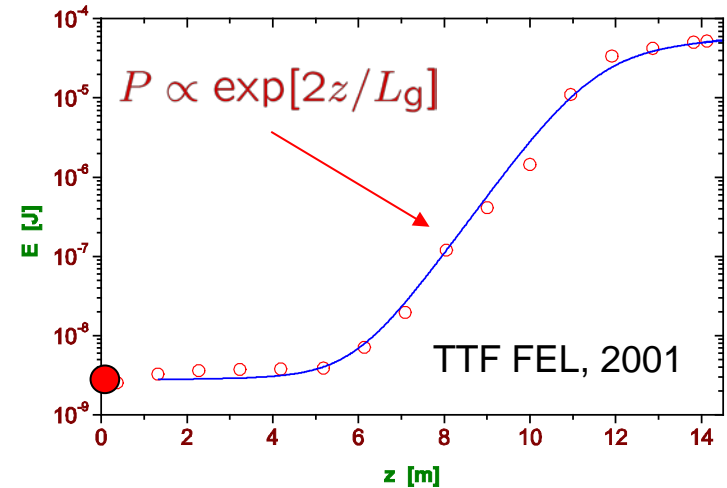
V. Ayvazyan et al., Phys. Rev. Lett. 88(2002)10482
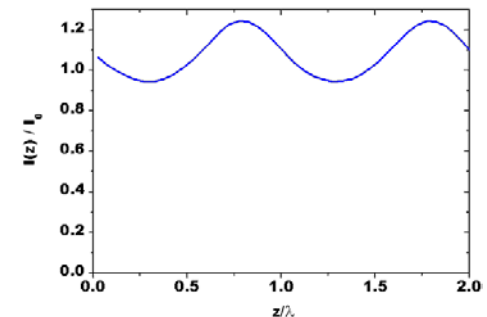
Coherent radiation of electron beams: Introduction. Example II: modulated electron bunch

Incoherent radiation power:

$$W_{\text{incoh}} \simeq \left[\frac{4\pi^2 eI}{\lambda}\right]\left[\frac{K^2}{1+K^2}\right] A_{\text{JJ}}^2 .$$

within the cone of half angle $\theta_{\text{con}} = \sqrt{1+K^2}/(\gamma\sqrt{N_{\text{w}}})$. Relative spectral bandwidth is $\Delta\lambda/\lambda \simeq 1/N_{\text{w}}$ near the resonance wavelength.

- Radiation energy of single electron into the central cone is $E_e \simeq 4\pi^2 e^2 K^2 A_{\text{JJ}}^2/[\lambda(1+K^2)]$. $A_{\text{JJ}} = 1$ for helical undulator, and $A_{\text{JJ}} = [J_0(Q) - J_1(Q)]$ for planar undulator. $J_n(Q)$ is a Bessel function of nth order, and $Q = K^2/2/(1+K^2)$.

- Wavepackets emitted by different electrons are not correlated, thus radiated power of the electron bunch with current I is just the radiation energy from a single electron multiplied by the electron flux I/e.

Radiation power of modulated electron beam:

$$W_{\text{mod}} = \left[\frac{\pi^2}{2}\right]\left[\frac{a_{\text{in}}^2 I^2 N_{\text{w}}}{c}\right]\left[\frac{K^2}{2+K^2}\right] A_{\text{JJ}}^2 \times F(N) .$$

$N = 2\pi\sigma^2/(\lambda\lambda_{\text{w}} N_{\text{w}})$ is Fresnel number. N_{w} is number of undulator periods

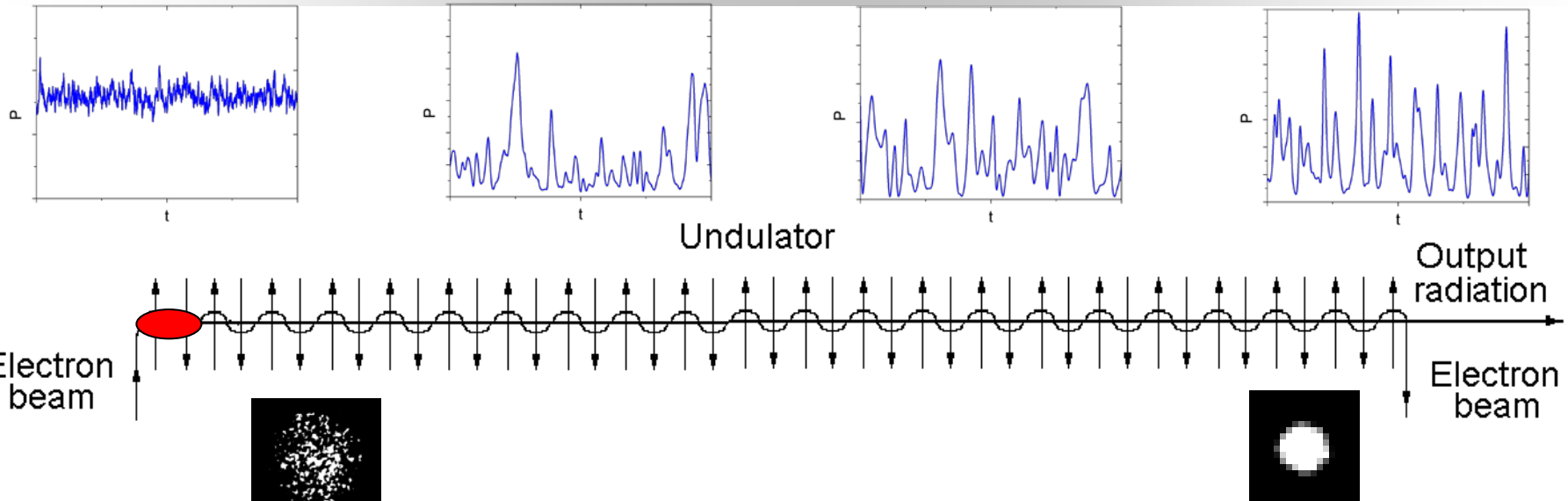$$F(N) = \frac{2}{\pi}\left[\arctan\left(\frac{1}{2N}\right) + N\ln\left(\frac{4N^2}{4N^2+1}\right)\right]$$

$$I(z) = I_0[1 + a_{\text{in}}\cos\omega(z/v_z - t)]$$

$$j(r) = I(z)exp(-r^2/2\sigma^2)/(\sqrt{2\pi}\sigma^2)$$

- Radiation power from modulated electron beam exceeds incoherent radiation when amplitude of modulation exceeds effective amplitude of shot noise:

$$a_{\text{in}} \gtrsim 1/\sqrt{N_\lambda N_{\text{w}}} , \qquad N_\lambda = I\lambda/(ec) .$$

- Radiation power from modulated electron beam holds potential to exceed the power of incoherent radiation by a factor of number of electrons in the volume of coherence, $N_{\text{c}} = N_\lambda \times N_{\text{w}}$.

E.L. Saldin, E.A. Schneidmiller and M.V. Yurkov, Nucl. Instrum. and Methods A539(2005)217

SASE FEL

Undulator

Output radiation

Electron beam

Electron beam

- When the electron beam enters the undulator, the presence of the beam modulation at frequencies close to the resonance frequency initiates the process of amplification.

- Fluctuations of current density in the electron beam are uncorrelated not only in time but in space, too. Thus, a large number of transverse radiation modes are excited when the electron beam enters the undulator.

- These radiation modes have different gain. As undulator length progresses, the high gain modes will predominate more and more and we can regard the XFEL as filter, in the sense that it filters from arbitrary radiation field those components corresponding to the high gain modes.

Qualitative look at the radiation properties
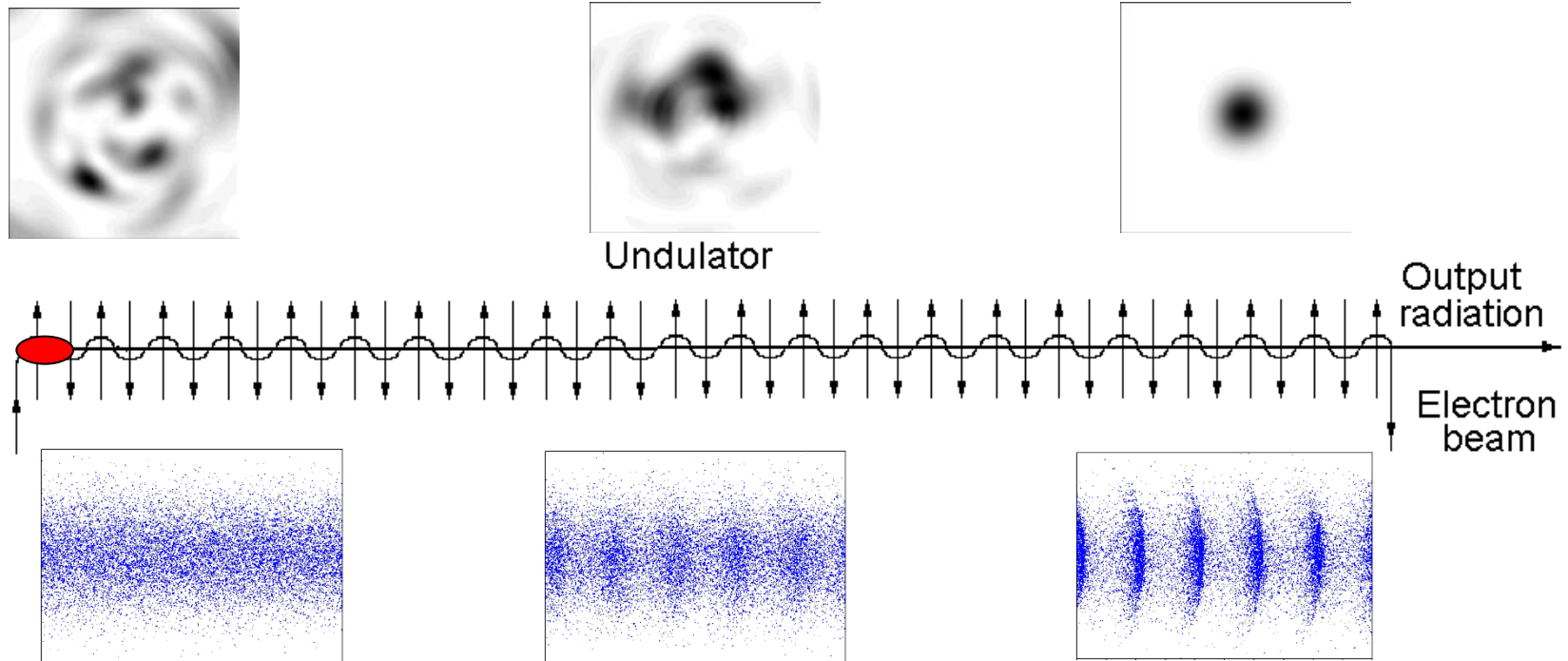
Undulator

- Longitudinal coherence is formed due to slippage effects (electromagnetic wave advances electron beam by one wavelength while electron beam passes one undulator period). Thus, typical figure of merit is relative slippage of the radiation with respect to the electron beam on a scale of field gain length ➔ coherence time.

- Transverse coherence is formed due to diffraction effects. Typical figure of merit is ratio of the diffraction expansion of the radiation on a scale of field gain length to the transverse size of the electron beam.

Qualitative look at the radiation properties

power
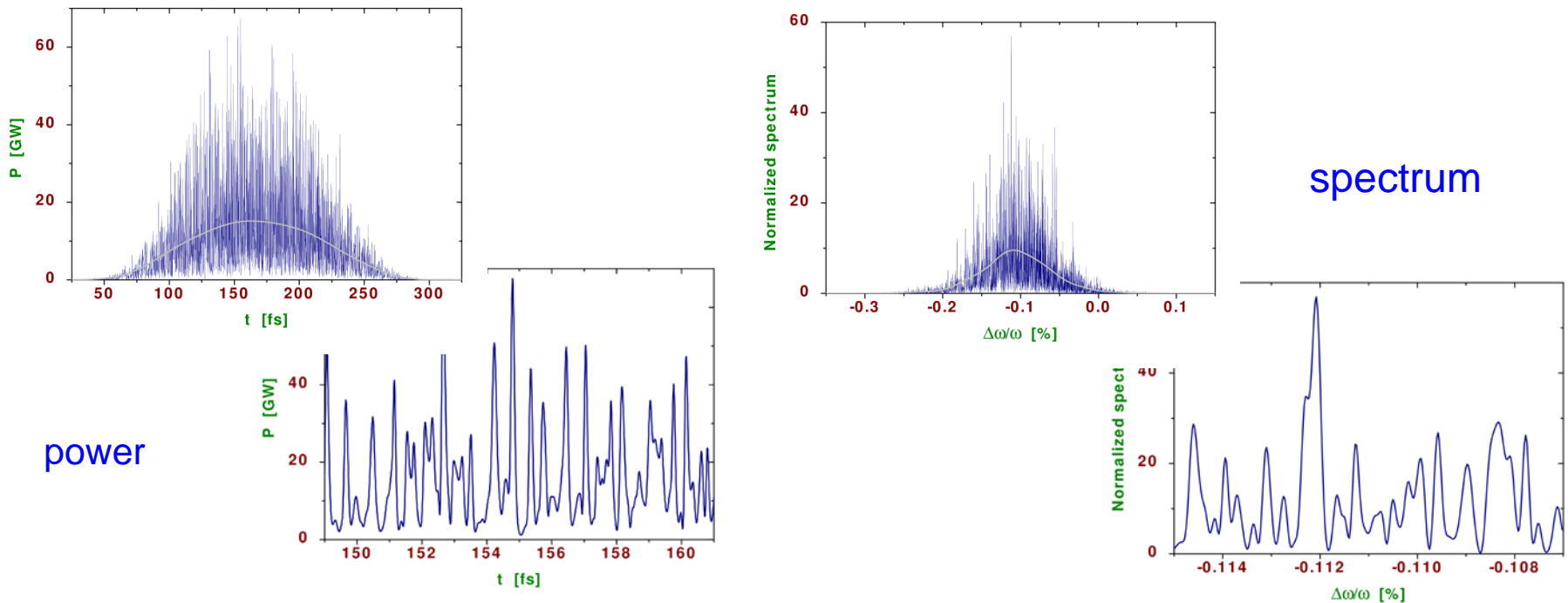
spectrum

- Radiation generated by SASE FEL consists of wavepackets (spikes). Typical duration of the spike is about coherence time τ_c.

- Spectrum also exhibits spiky structure. Spectrum width is inversely proportional to the coherence time, $\Delta\omega \sim 1/\tau_c$, and typical width of a spike in a spectrum is inversely proportional to the pulse duration T.

- Amplification process selects narrow band of the radiation, coherence time is increased, and spectrum is shrinked. Transverse coherence is improved as well due to the mode selection process.

M.V. Yurkov, Coherence properties of the radiation from SASE FEL, CERN Accelerator School on FELs and ERLs, 31 May – 10 June, 2016

SASE FEL: Group velocity of wavepackets

- Group velocity of wavepacket (spike) in the linear regime (1D asymptote):

$$\frac{1}{v_g} = \frac{dk}{d\omega} = \left[c \left(1 - \frac{1}{3\gamma_z^2} \right) \right]^{-1} .$$

- The relative slippage of the wavepackets (spikes) with respect to the electron beam in the linear regime is three times less than the kinematic slippage $c - \bar{v}_z = c/(2\gamma_z^2)$:

$$\frac{v_g - \bar{v}_z}{c - \bar{v}_z} = \frac{1}{3} .$$

- This effect takes place due to the dispersive properties of the active medium — the electron beam in the undulator. The effect of slippage suppression is even stronger when diffraction effects are taken into account (see left plot).

- In the nonlinear regime interaction of the wave with the electron beam is not so strong, and group velocity of spikes approach to the velocity of light (see right plot).
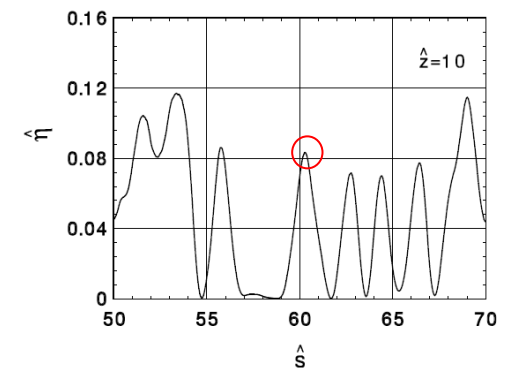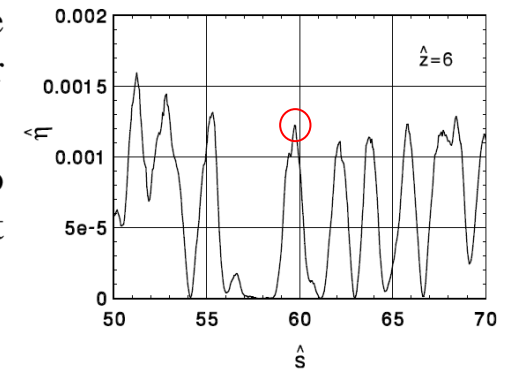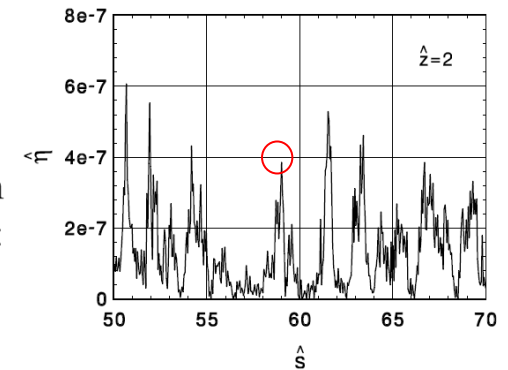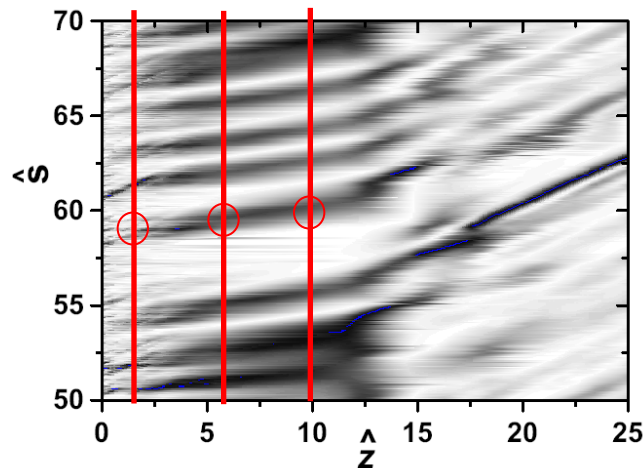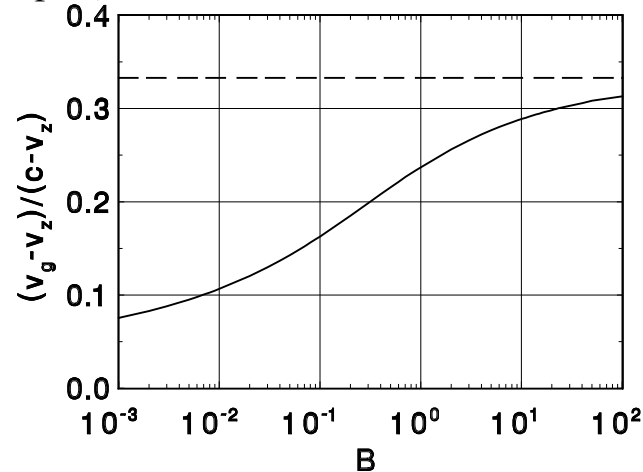
SASE FEL

- Radiation from SASE FEL is statistical object, thus statistical approach needs to be applied for analysis of the properties of the radiation from SASE FEL:

  - Nature of statistics.
  - Description in terms of correlation functions and probability distribution functions.
  - Description of averaged characteristics (ensemble averaging).

- Physical effects related to coherence properties:

  - Longitudinal coherence: slippage effects – can be studied in the framework of 1D approximation
  - Transverse coherence: diffraction effects – can be studied in the framework of full 3D model only.

- The first order time correlation function and coherence time:

$$g_1(\vec{r}, t - t') = \frac{\langle \tilde{E}(\vec{r}, t) \tilde{E}^*(\vec{r}, t') \rangle}{\left[\langle | \tilde{E}(\vec{r}, t) |^2 \rangle \langle | \tilde{E}(\vec{r}, t') |^2 \rangle \right]^{1/2}} , \qquad \tau_c = \int_{-\infty}^{\infty} |g_1(\tau)|^2 \, d\tau .$$

- The first-order transverse correlation function and degree of transverse coherence:

$$\gamma_1(\vec{r}_\perp, \vec{r}\prime_\perp, z, t) = \frac{\langle \tilde{E}(\vec{r}_\perp, z, t) \tilde{E}^*(\vec{r}\prime_\perp, z, t) \rangle}{\left[\langle | \tilde{E}(\vec{r}_\perp, z, t)|^2 \rangle \langle | \tilde{E}(\vec{r}\prime_\perp, z, t)|^2 \rangle \right]^{1/2}} .$$

$$\zeta = \frac{\int \int |\gamma_1(\vec{r}_\perp, \vec{r}\prime_\perp)|^2 \langle I(\vec{r}_\perp) \rangle \langle I(\vec{r}\prime_\perp) \rangle \, d\vec{r}_\perp \, d\vec{r}\prime_\perp}{[\int \langle I(\vec{r}_\perp) \rangle \, d\vec{r}_\perp]^2} .$$

- Degeneracy parameter – the number of photons per mode (coherent state):

$$\delta = \dot{N}_{ph} \tau_c \zeta .$$

- Peak brilliance is defined as a transversely coherent spectral flux:

$$B_r = \frac{\omega \, d\dot{N}_{ph}}{d\omega} \frac{\zeta}{\left(\frac{\lambda}{2}\right)^2} = \frac{4\sqrt{2}c}{\lambda^3} \delta .$$

Statistics and probability distributions

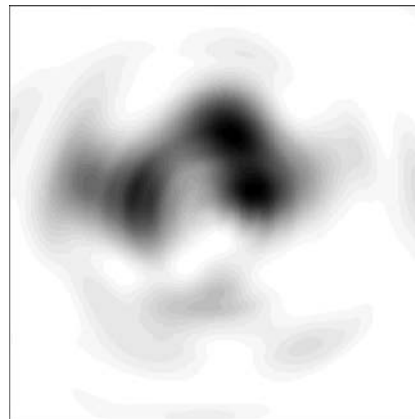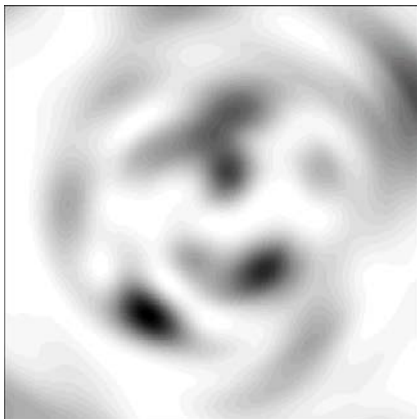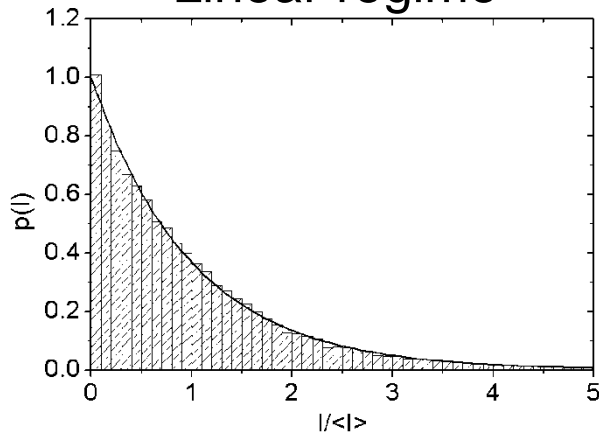$z = 0.1\ z_{sat}$ $z = 0.5\ z_{sat}$ $z = z_{sat}$
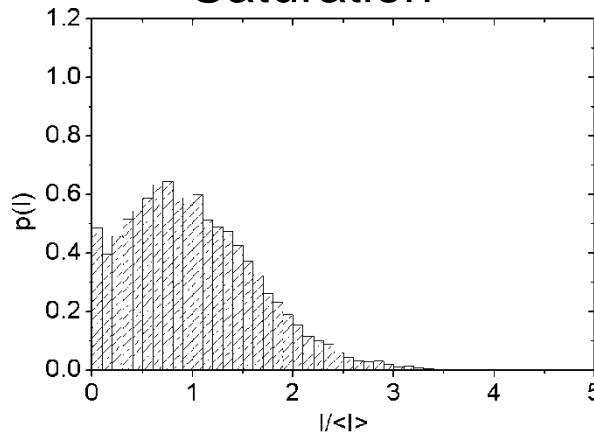
- Transverse (bottom) and longitudinal (top) distributions of the radiation intensity exhibit rather chaotic behaviour.
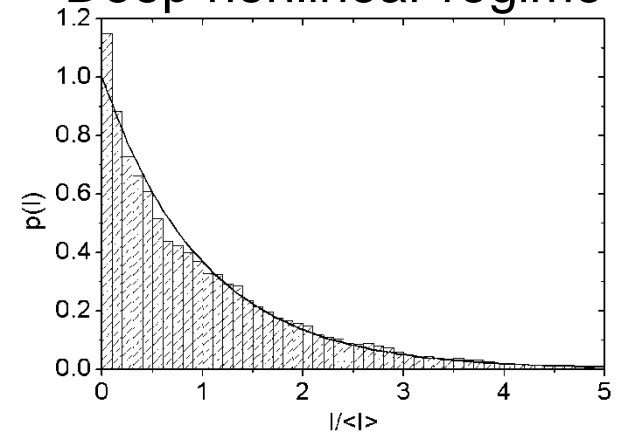
M.V. Yurkov, Coherence properties of the radiation from SASE FEL, CERN Accelerator School on FELs and ERLs, 31 May – 10 June, 2016

Statistics and probability distributions
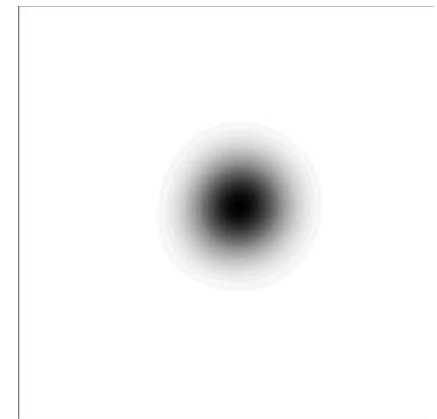
Linear regime

Saturation

Deep nonlinear regime

- Probability distributions of the instantaneous power density (top) and of the instantaneous radiation power (bottom) look more elegant and seem to be described by simple functions.

Statistics and probability distributions
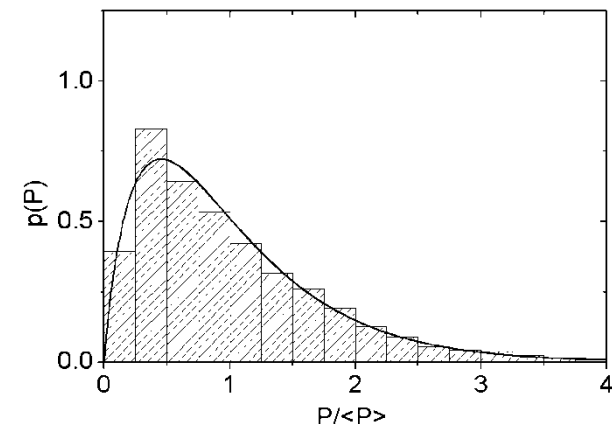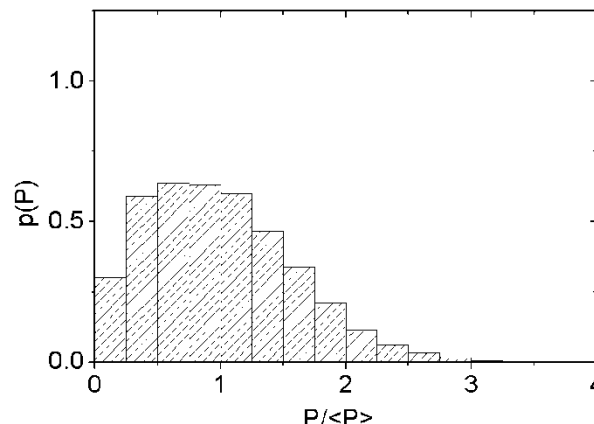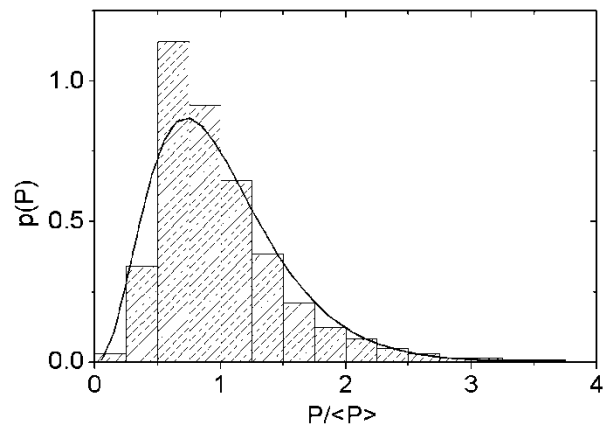
- The origin of this fundamental simplicity relates to the properties of the electron beam. The shot noise in the electron beam has a statistical nature that significantly influences characteristics of the output radiation from a SASE FEL.

- Fluctuations of the electron beam current density serve as input signals in a SASE FEL. These fluctuations always exist in the electron beam due to the effect of shot noise. Initially fluctuations are not correlated in space and time, but when the electron beam enters the undulator, beam modulation at frequencies close to the resonance frequency of the FEL amplifier initiates the process of the amplification of coherent radiation.

- Electron beam current is $I(t) = (-e)\Sigma_{k=1}^{N}\delta(t - t_k)$, and its Fourier harmonic is just a sum of complex phasors:

$$\bar{I}(\omega) = \int_{-\infty}^{\infty} e^{i\omega t} I(t)dt = (-e)\sum_{k=1}^{N} e^{i\omega t_k}$$

- Thus, we deal with gaussian statistical process. FEL amplifier operating in the linear regime is just linear filter, $\bar{E}(\omega) = H_A(\omega - \omega_0)\bar{I}(\omega)$, which does not change statistics.

E.L. Saldin, E.A. Schneidmiller, M.V. Yurkov, The Physics of Free Electron Lasers

M.V. Yurkov, Coherence properties of the radiation from SASE FEL, CERN Accelerator School on FELs and ERLs, 31 May – 10 June, 2016

SASE FEL, linear regime: general features

- For gaussian random process any integral of the power density, $\mathcal{I}$, fluctuates in accordance with the gamma distribution:

$$p(\mathcal{I}) = \frac{M^M}{\Gamma(M)} \left(\frac{\mathcal{I}}{\langle\mathcal{I}\rangle}\right)^{M-1} \frac{1}{\langle\mathcal{I}\rangle} \exp\left(-M\frac{\mathcal{I}}{\langle\mathcal{I}\rangle}\right) ,$$
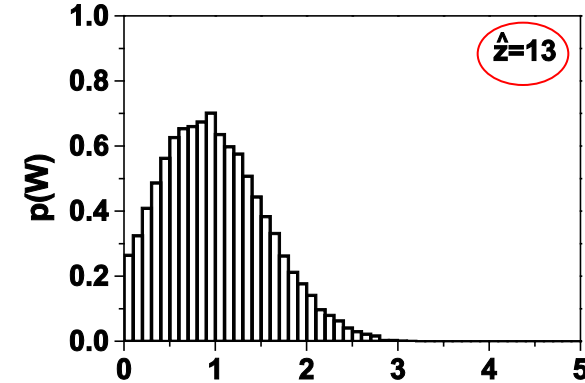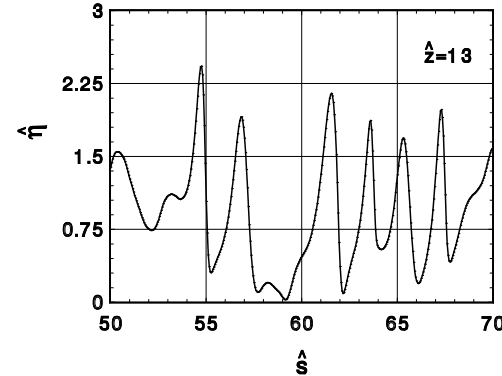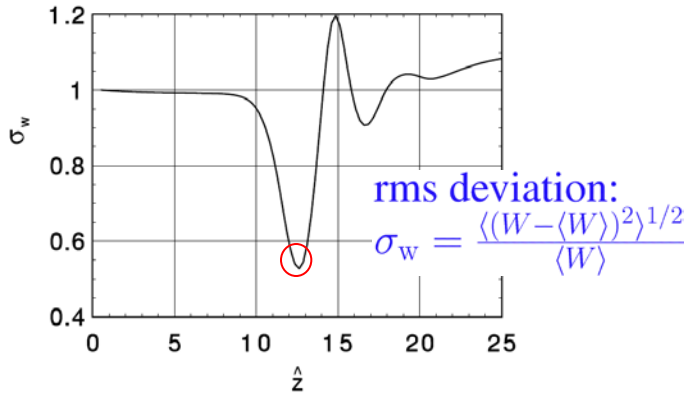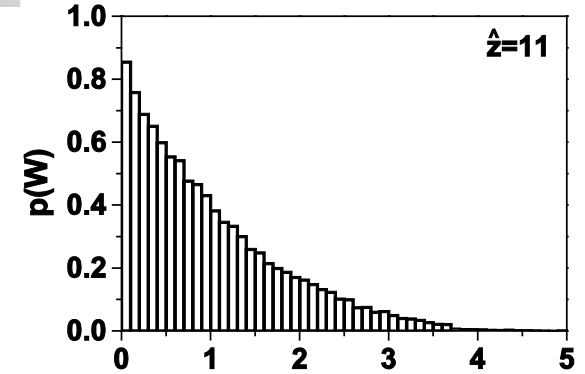
where $\Gamma(M)$ is the gamma function with argument M,

$$M = \frac{1}{\sigma_{\mathrm{P}}^2} , \qquad \sigma_{\mathrm{P}}^2 = \langle(\mathcal{I} - \langle\mathcal{I}\rangle)^2\rangle/\langle\mathcal{I}\rangle^2 .$$
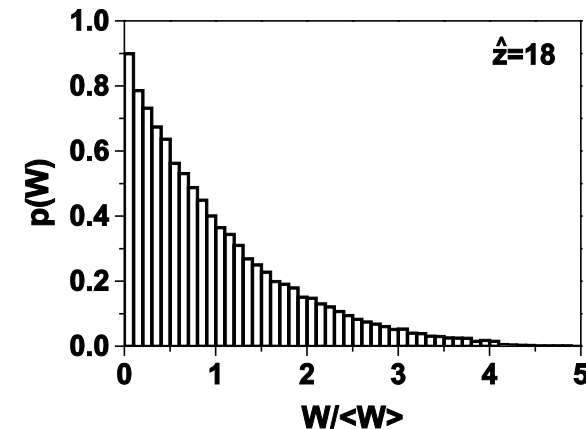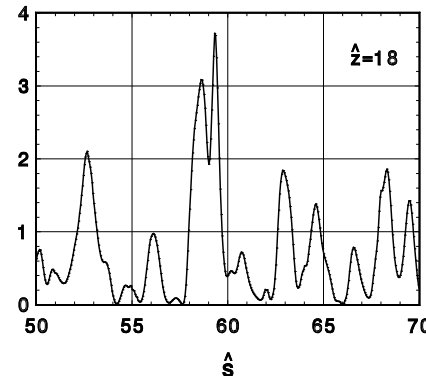
- The parameter M can be interpreted as the average number of "degrees of freedom" or "modes".

- For instance, if the integral $\mathcal{I}$ is the radiation energy, $\mathcal{I} = E_{\mathrm{rad}} = \int I\,dt\,d\vec{r}_\perp$, then parameter M is associated with the total number of modes in the radiation pulse, i.e. longitudinal and transverse modes. If the integral is the radiation power, $\mathcal{I} = P = \int I\,d\vec{r}_\perp$, then parameter M is the number of transverse modes, $M_\perp$. Thus, it becomes clear that the relative dispersion of the radiation power directly relates to the coherence properties of the SASE FEL operating in the linear regime.
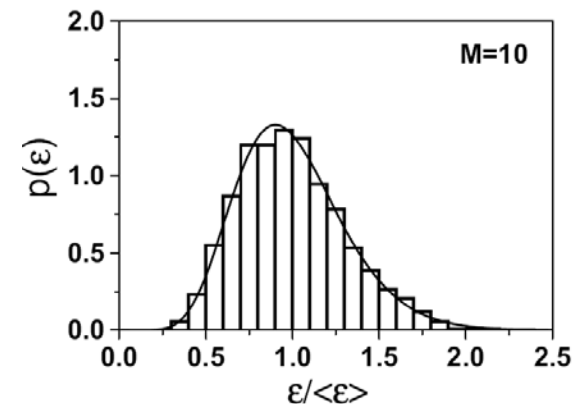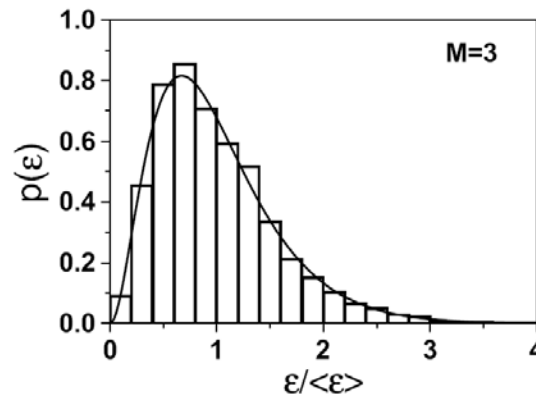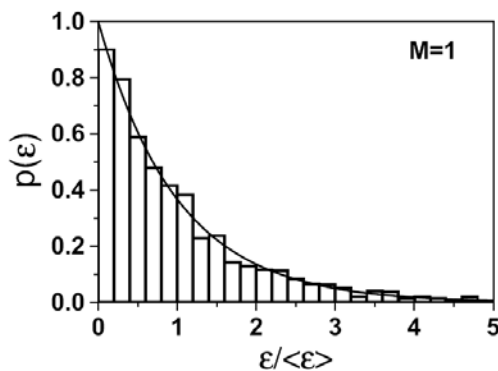
- Amplification process passes stage of exponential growth (linear regime), and then enters nonlinear regime.
- Probability distributions follow negative exponential distribution in linear and deep nonlinear regime. Minimum of fluctuations occurs in the saturation.

The rms deviation:
$$\sigma_{\mathrm{w}} = \frac{\langle (W - \langle W \rangle)^2 \rangle^{1/2}}{\langle W \rangle}$$

SASE FEL: time correlation functions and the coherence time

- The first, the second order time correlation functions, and coherence time:

$$g_1(t - t') = \frac{< \tilde{E}(t)\tilde{E}^*(t') >}{\left[<| \tilde{E}(t) |^2><| \tilde{E}(t') |^2>\right]^{1/2}} ,$$

$$g_2(t - t') = \frac{<| \tilde{E}(t) |^2 | \tilde{E}(t') |^2>}{<| \tilde{E}(t) |^2><| \tilde{E}(t') |^2>}$$

$$\tau_c = \int_{-\infty}^{\infty} | g_1(\tau) |^2 \, d\tau$$
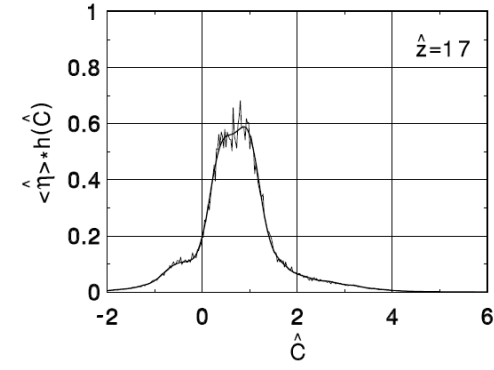
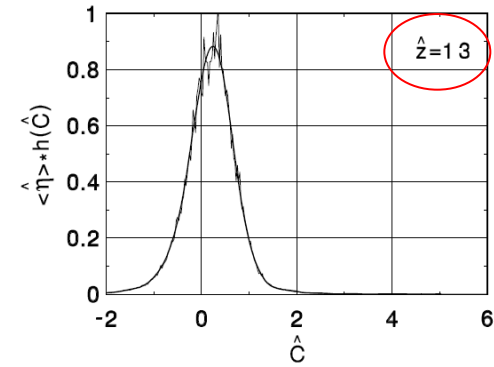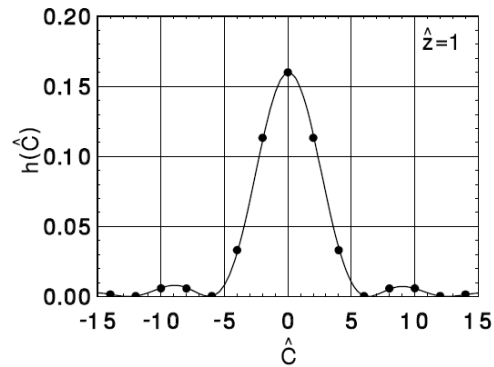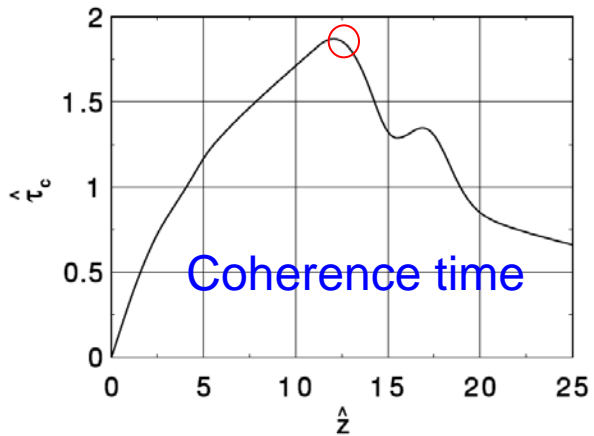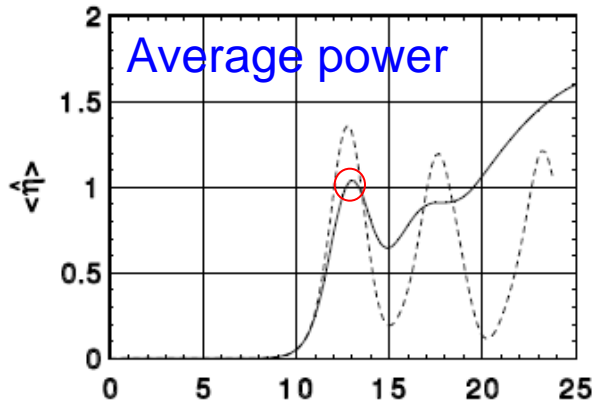- High gain linear regime:

$$g_1(\tau) = \exp\left(-\frac{9\rho^2\omega_0^2\tau^2}{\sqrt{3}\hat{z}}\right) ,$$

$$g_2(t - t') = 1 + | g_1(t - t') |^2 = 1 + \exp\left(-\frac{18\rho^2\omega_0^2\tau^2}{\sqrt{3}\hat{z}}\right) .$$

$$\tau_c = \sqrt{\frac{\sqrt{3}\pi\hat{z}}{18}}\frac{1}{\rho\omega_0}$$

Maximum coherence time is achieved in the end of high gain linear regime.

SASE FEL: Evolution of spectrum

Average power

Coherence time
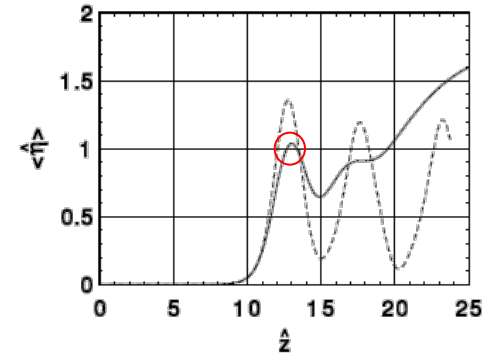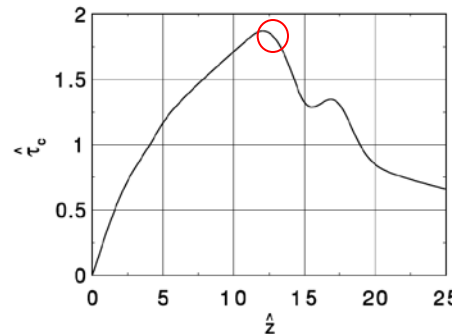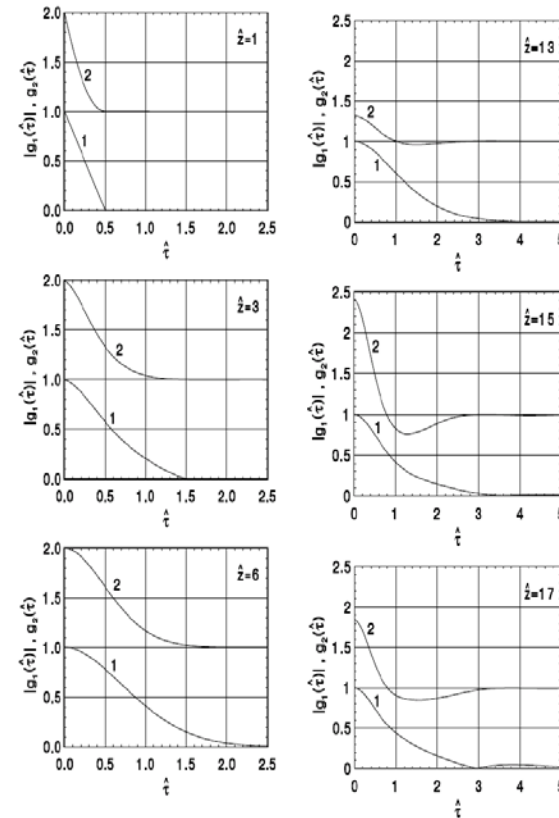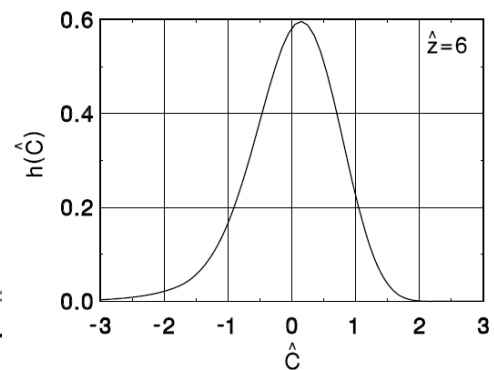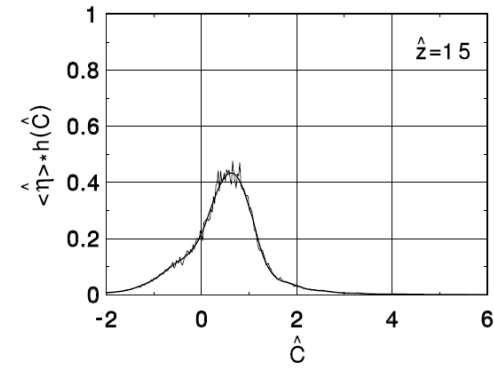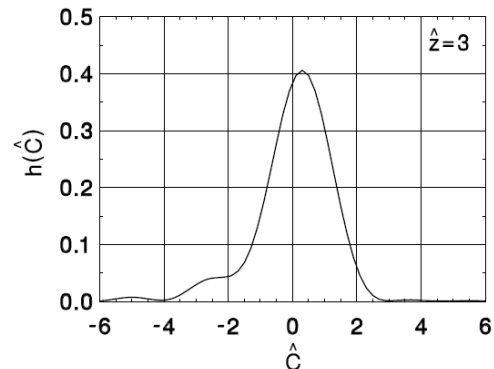
- High gain linear regime:

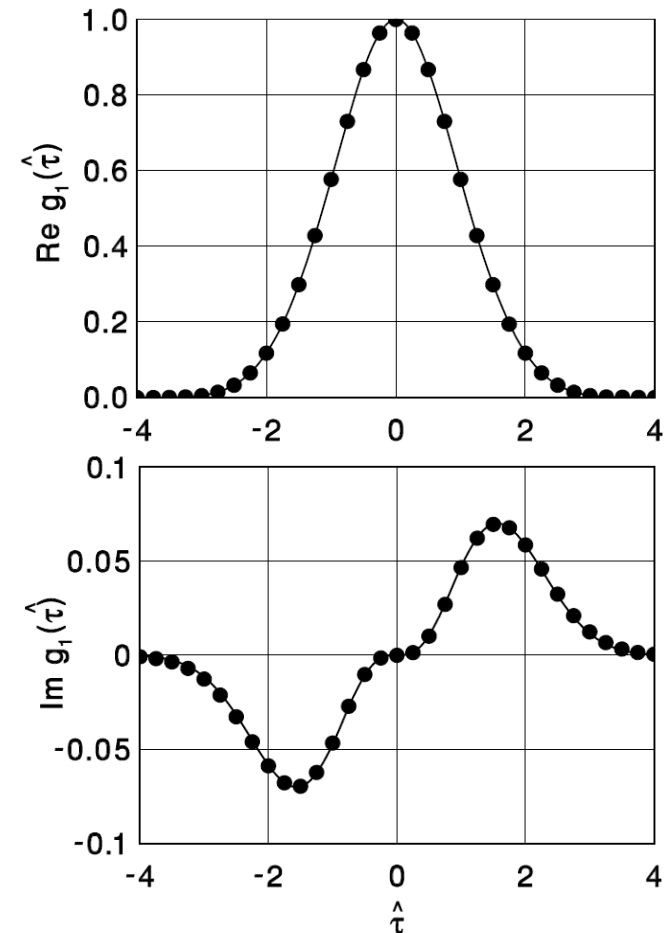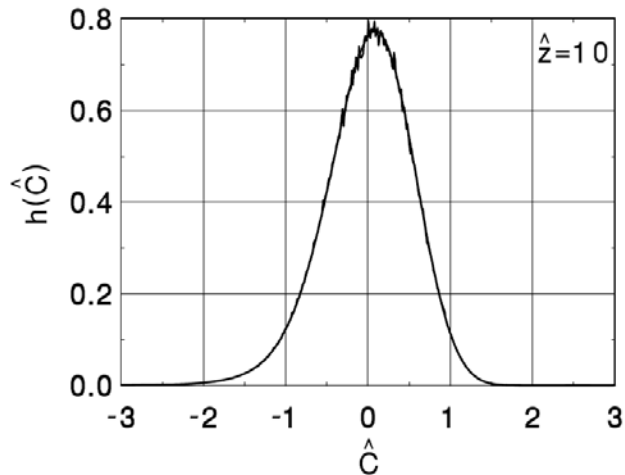$$\sigma_\omega = \frac{\sqrt{\pi}}{\tau_c} = \rho\omega_0\sqrt{\frac{18}{\sqrt{3}\hat{z}}}$$

- Minimum spectrum width is achieved in the end of the high gain linear regime. It is increased in the noninear regime due to the growth of sidebands in the nonlinear media.

- The first order time correlation function

$$g_1(t - t') = \frac{< \tilde{E}(t)\tilde{E}^*(t') >}{\left[<| \tilde{E}(t) |^2><| \tilde{E}(t') |^2>\right]^{1/2}},$$

- Wiener-Khintchine theorem: spectral power of the process and the first order time correlation function form a Fourier pair:

$$\frac{| H_A(\Delta\omega) |^2}{\int\limits_{-\infty}^{\infty} d(\Delta\omega) | H_A(\Delta\omega) |^2} = \frac{1}{2\pi} \int\limits_{-\infty}^{\infty} d\tau\, g_1(\tau) \exp(-i\Delta\omega\tau)$$

Linear regime

Radiation from SASE FEL operating in the high gain linear regime possesses all the features of completely chaotic polarized light:

- The higher order correlation functions are expressed via the first order correlation function
- The probability density distribution of the instantaneous radiation power follows the negative exponential distribution
- The probability density function of the finite-time integrals of the instantaneous power and of the radiation energy after monochromator follow the gamma distribution

## Nonlinear regime

- Maximum spectral brightness and coherence time is achieved in the saturation.
- At further increase of the undulator length average power continues to grow; coherence time decreases; the width of the spectrum increases.
- Distribution of the instantaneous power changes significantly near the saturation point, but tends to the negative exponential law in the deep nonlinear regime.

Probability distribution of the energy in the radiation pulse

Probability distribution of the energy after narrow band monochromator
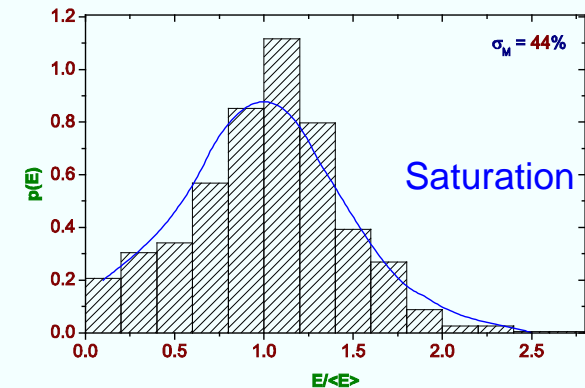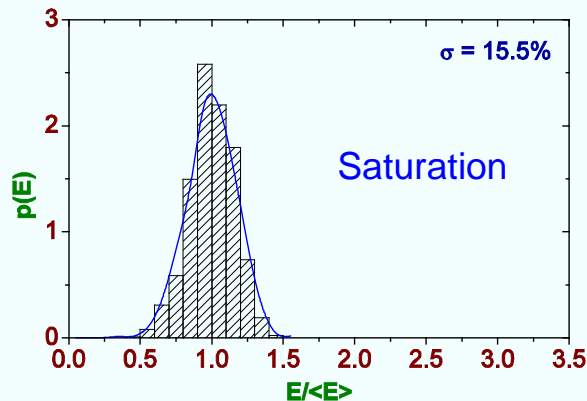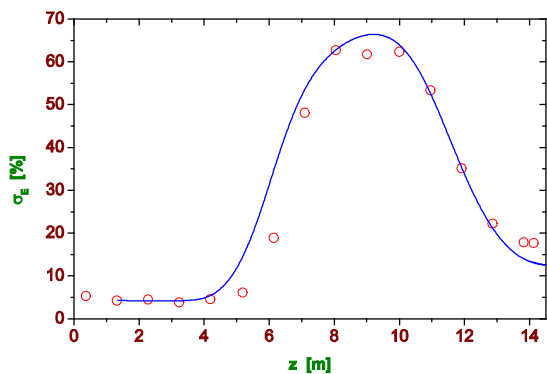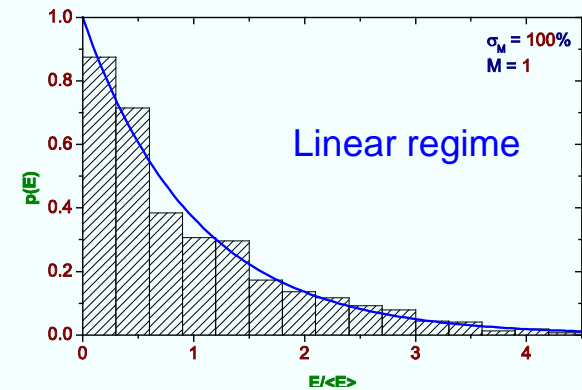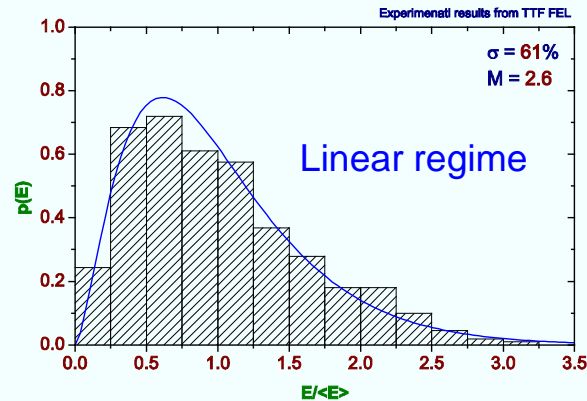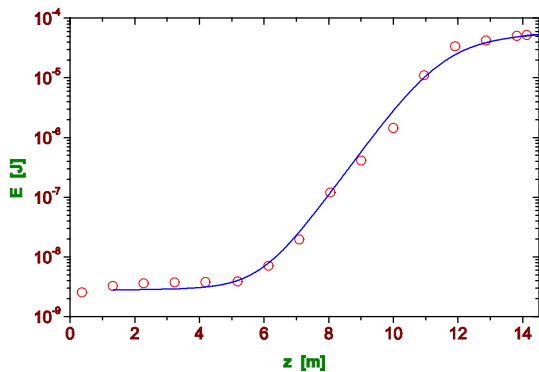
• FEL parameter ρ and number of cooperating electrons N_c:

$$\rho = \frac{\lambda_w}{4\pi}\left[\frac{4\pi^2 j_0 K^2 A_{JJ}^2}{I_A \lambda_w \gamma^3}\right]^{1/3} , \qquad N_c = I/(e\rho\omega) .$$

• Main properties of SASE FEL in the saturation can be quickly estimated in terms of ρ and N_c:

The field gain length : $\quad L_g \sim \lambda_w/(4\pi\rho)$,

Saturation length : $\quad L_{sat} \sim 10 \times L_g$,

Effective power of shot noise : $\quad \dfrac{W_{sh}}{\rho W_b} \simeq \dfrac{3}{N_c\sqrt{\pi \ln N_c}}$,

Saturation efficiency : $\quad \rho$,

The power gain at saturation : $\quad G \simeq \dfrac{1}{3}N_c\sqrt{\pi \ln N_c}$,

Coherence time at saturation : $\quad \tau_c \simeq \dfrac{1}{\rho\omega}\sqrt{\dfrac{\pi \ln N_c}{18}}$,

Spectrum bandwidth : $\quad \sigma_\omega \simeq \rho\omega\sqrt{\dfrac{18}{\ln N_c}}$.

I. Start-up of the FEL process from shot noise: SASE FEL.

II. Longitudinal coherence (temporal and spectral properties). Statistics.

III. Transverse coherence.

IV. Higher harmonics.

Strict definitions of statistical characteristics

- The first order time correlation function and coherence time:

$$g_1(\vec{r}, t - t') = \frac{\langle \tilde{E}(\vec{r}, t)\tilde{E}^*(\vec{r}, t')\rangle}{\left[\langle | \tilde{E}(\vec{r}, t) |^2\rangle\langle | \tilde{E}(\vec{r}, t') |^2\rangle\right]^{1/2}} , \qquad \tau_c = \int\limits_{-\infty}^{\infty} |g_1(\tau)|^2 \, \mathrm{d}\tau .$$

- The first-order transverse correlation function and degree of transverse coherence:

$$\gamma_1(\vec{r}_\perp, \vec{r}\prime_\perp, z, t) = \frac{\langle \tilde{E}(\vec{r}_\perp, z, t)\tilde{E}^*(\vec{r}\prime_\perp, z, t)\rangle}{\left[\langle |\tilde{E}(\vec{r}_\perp, z, t)|^2\rangle\langle |\tilde{E}(\vec{r}\prime_\perp, z, t)|^2\rangle\right]^{1/2}} .$$

$$\zeta = \frac{\int\int |\gamma_1(\vec{r}_\perp, \vec{r}\prime_\perp)|^2\langle I(\vec{r}_\perp)\rangle\langle I(\vec{r}\prime_\perp)\rangle \, \mathrm{d}\vec{r}_\perp \, \mathrm{d}\vec{r}\prime_\perp}{[\int\langle I(\vec{r}_\perp)\rangle \, \mathrm{d}\vec{r}_\perp]^2} .$$
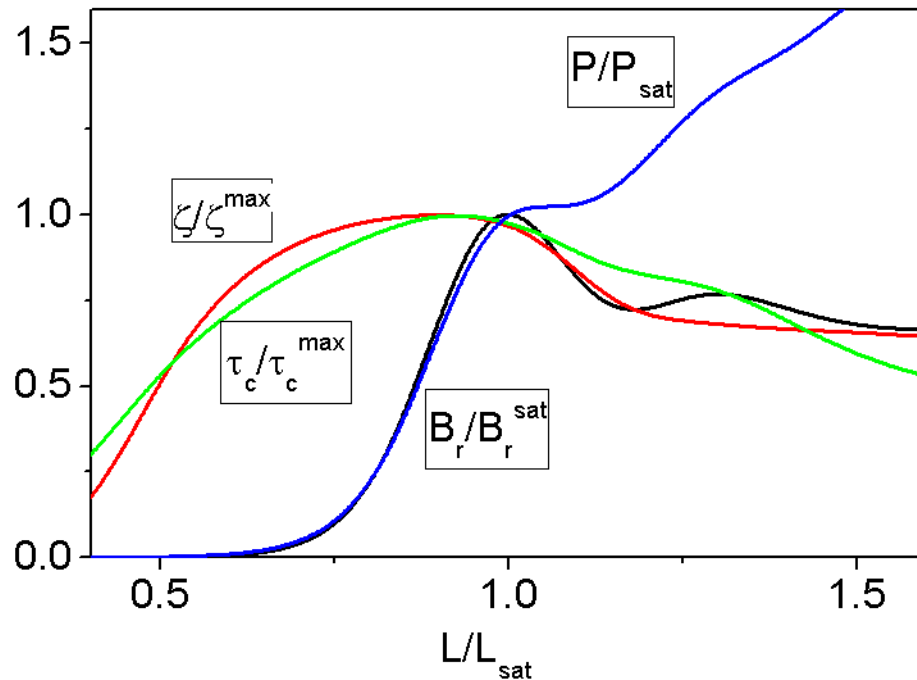
- Degeneracy parameter – the number of photons per mode (coherent state):

$$\delta = \dot{N}_{ph}\tau_c\zeta .$$

- Peak brilliance is defined as a transversely coherent spectral flux:

$$B_r = \frac{\omega \, \mathrm{d}\dot{N}_{ph}}{\mathrm{d}\omega} \frac{\zeta}{\left(\frac{\lambda}{2}\right)^2} = \frac{4\sqrt{2}c}{\lambda^3} \delta .$$

# Qualitative look at the evolution of the radiation properties in XFEL

Radiation power

Brilliance

Degree of transverse coherence

Coherence time

- Radiation power continues to grow along the undulator length.
- Brilliance reaches maximum value at the saturation point.
- Degree of transverse coherence and coherence time reach their maximum values in the end of exponential regime.

Qualitative look at the transverse coherence
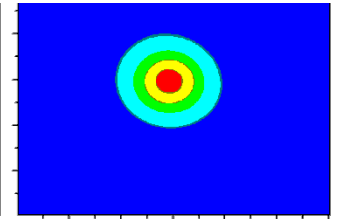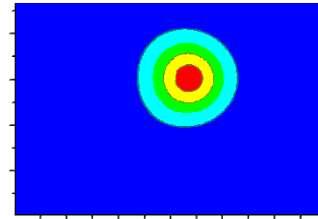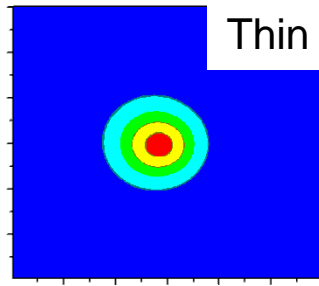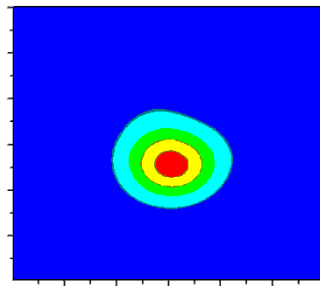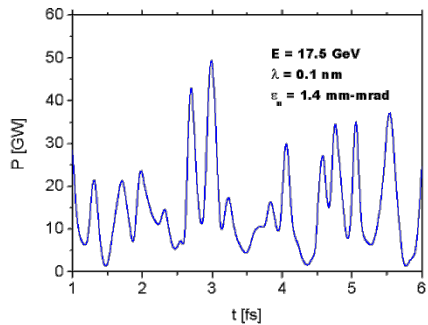
Thin (diffraction limited) electron beam
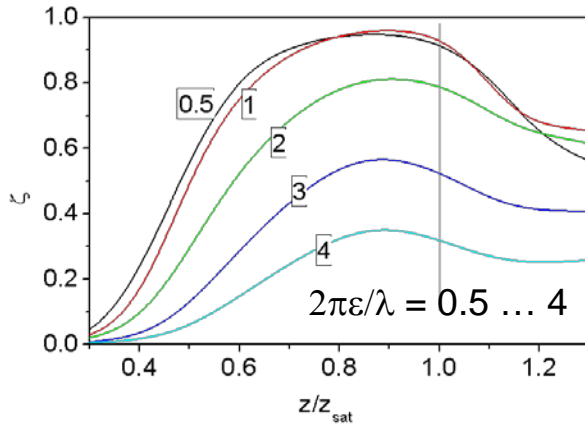
- Undulator length to saturation is limited (9 to 10 field gain length for X-ray FELs).

- In the case of wide electron beam (with transverse size larger than diffraction expansion of the radiation on the scale of the field gain length) , the degree of transverse coherence degrades due to poor mode selection.
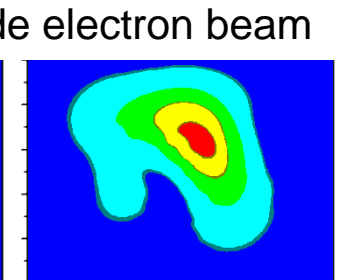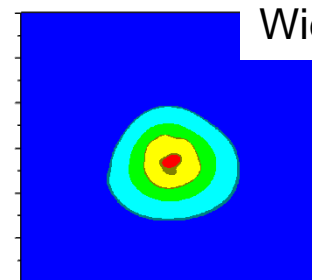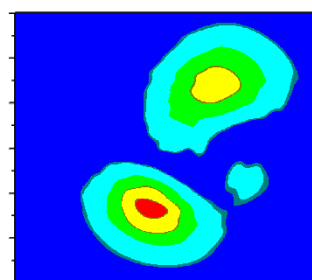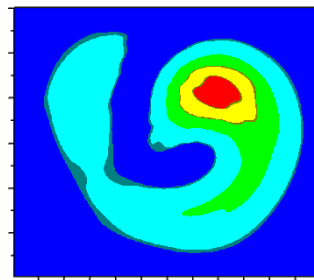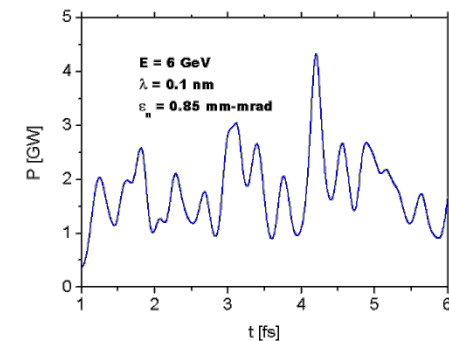
$2\pi\varepsilon/\lambda = 0.5 \dots 4$

Wide electron beam

Transverse coherence

Degree of transverse coherence

ζ

0.5 1 2 3 4

$2\pi\varepsilon/\lambda = 0.5 \ldots 4$

z/z_{sat}

z-s intensity distribution

$s = \rho\omega(z/V_z - t)$

z/z_{sat}
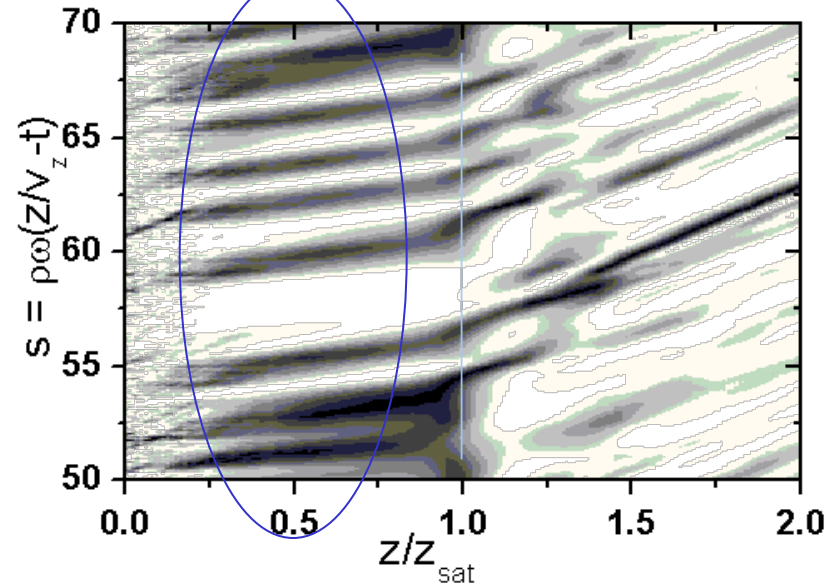
$$E_x + iE_y = \int d\omega \exp[i\omega(z/c - t)] \times \sum_{n,k} A_{nk}(\omega, z)\Phi_{nk}(r, \omega)\exp[\Lambda_{nk}(\omega)z + in\phi]$$

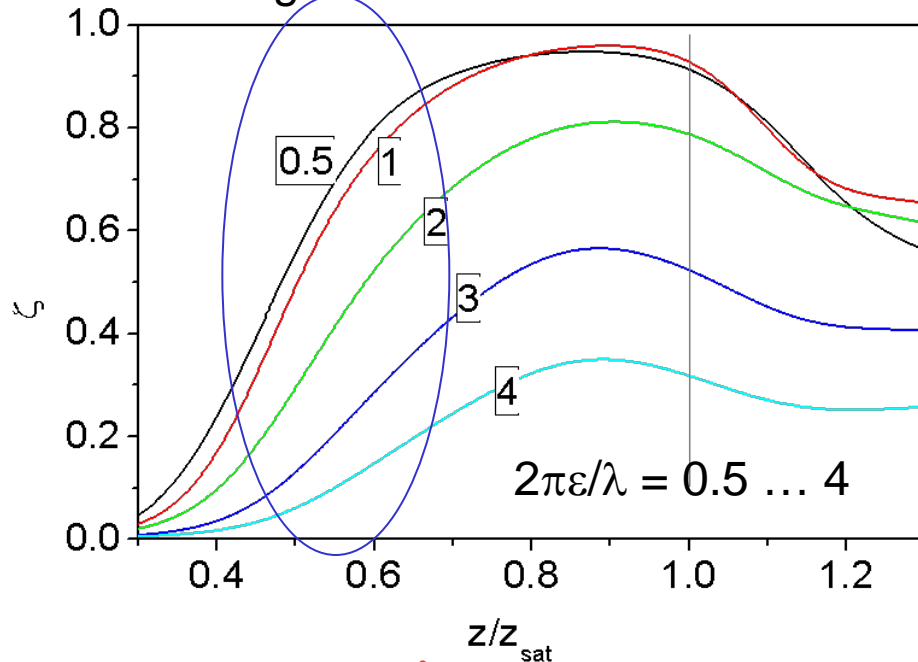- In the case of large emittance the degree of transverse coherence degrades due to poor mode selection.

- For small emittances the degree of transverse coherence visibly differs from unity. This happens due to poor longitudinal coherence: radiation spikes move forward along the electron beam, and interact with those parts of the beam which have different amplitude/phase.

- Longitudinal coherence develops slowly with the undulator length thus preventing full transverse coherence.

E.L. Saldin, E.A. Schneidmiller, M.V. Yurkov, Opt. Commun. 186(2000)185

$$E_x + iE_y = \int d\omega \exp[i\omega(z/c - t)] \times \sum_{n,k} A_{nk}(\omega, z)\Phi_{nk}(r, \omega)\exp[\Lambda_{nk}(\omega)z + in\phi]$$
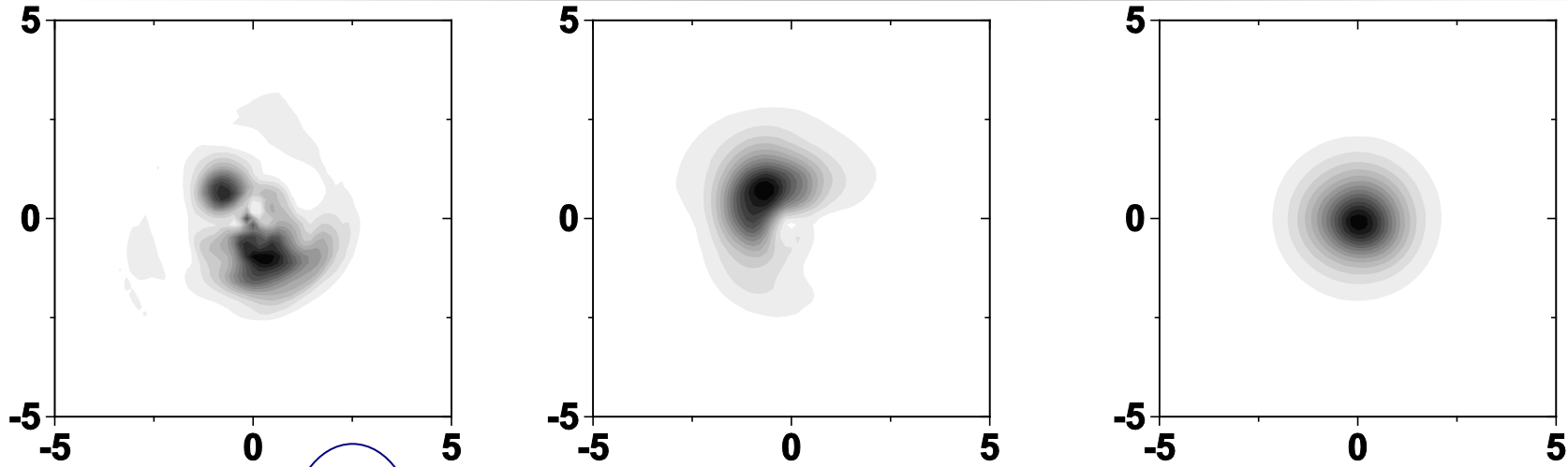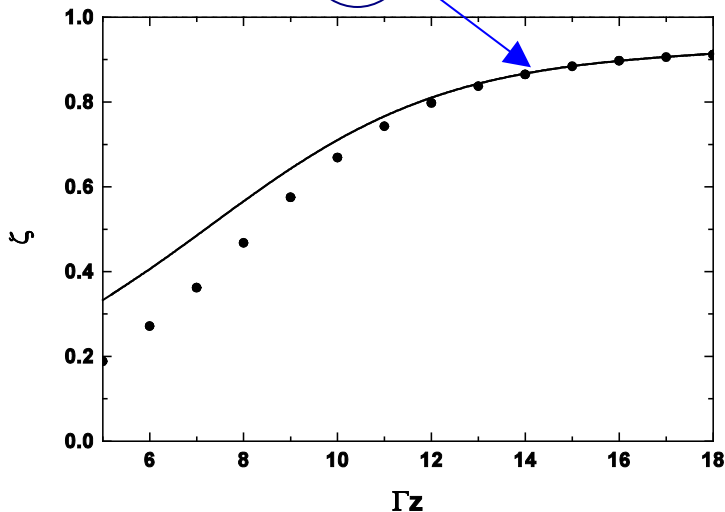

Even after finishing the transverse mode selection process the degree of transverse coherence of the radiation from SASE FEL visibly differs from unity. This is consequence of the interdependence of the longitudinal and transverse coherence. The SASE FEL has poor longitudinal coherence which develops slowly with the undulator length thus preventing a full transverse coherence.

Transverse coherence

Degree of transverse coherence

$2\pi\varepsilon/\lambda = 0.5 \ldots 4$
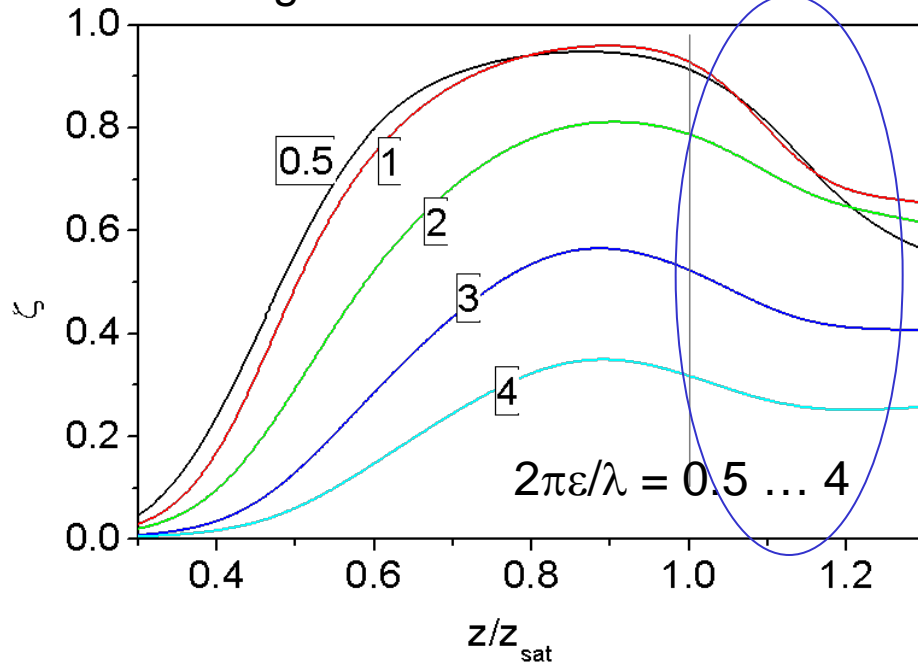
z-s intensity distribution
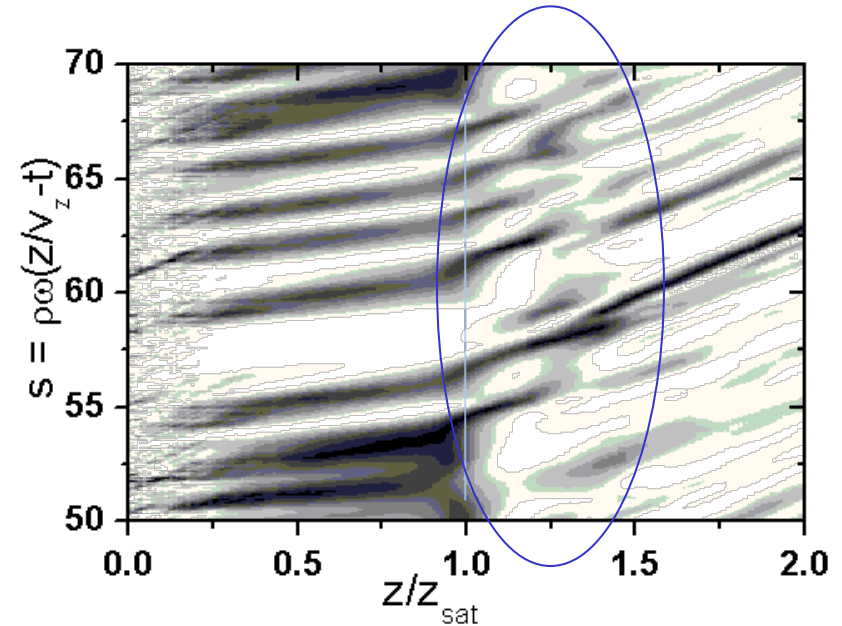
- Poor longitudinal coherence is also responsible for the fast degradation of the transverse coherence in the nonlinear regime.
- In the linear exponential regime group velocity of spikes is visibly less than the velocity of light due to strong interaction with the electron beam. In the nonlinear regime group velocity of spikes approaches velocity of light due to weak interaction with the electron beam.
- Radiation spikes move forward faster along the electron beam and start to interact with those parts of the beam which were formed due to interaction with different wavepackets.
- This process develops on the scale of the field gain length.

- In the linear high-gain limit the radiation emitted by the electron beam in the undulator can be represented as a set of modes:

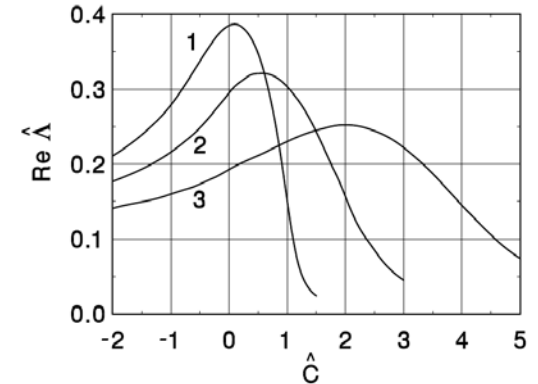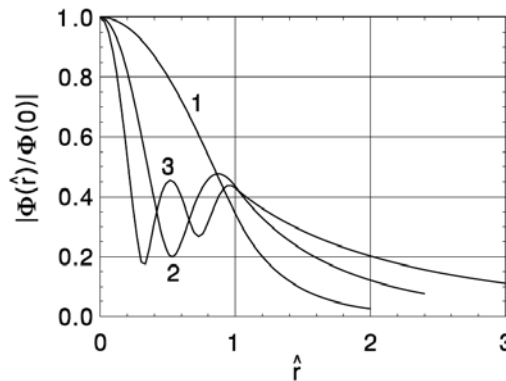$$E_{\mathrm{x}} + iE_{\mathrm{y}} = \int d\omega \exp[i\omega(z/c - t)] \times \sum_{n,k} A_{nk}(\omega, z)\Phi_{nk}(r, \omega)\exp[\Lambda_{nk}(\omega)z + in\phi] .$$

- A large number of transverse radiation modes are excited when the electron beam enters the undulator.

$$\left[\frac{d^2}{d\hat{r}^2} + \frac{1}{\hat{r}}\frac{d}{d\hat{r}} - \frac{n^2}{\hat{r}^2} + 2iB\hat{\Lambda}\right]\Phi_n(\hat{r})$$

$$= -4\int_0^{\infty} d\hat{r}'\hat{r}'\{\Phi_n(\hat{r}') \tag{4}$$

$$+ \frac{\hat{\Lambda}_{\mathrm{p}}^2}{2}\left[\frac{d^2}{d\hat{r}'^2} + \frac{1}{\hat{r}'}\frac{d}{d\hat{r}'} - \frac{n^2}{\hat{r}'^2} + 2iB\hat{\Lambda}\right]\Phi_n(\hat{r}')\}$$

$$\times \int_0^{\infty} d\zeta\frac{\zeta}{\sin^2(\hat{k}_\beta\zeta)}\exp\left[-\frac{\hat{\Lambda}_T^2\zeta^2}{2} - (\hat{\Lambda} + i\hat{C})\zeta\right]$$

$$\times \exp\left[-\frac{(1 - iB\hat{k}_\beta^2/2)(\hat{r}^2 + \hat{r}'^2)}{\sin^2(\hat{k}_\beta\zeta)}\right]$$

$$\times I_n\left[\frac{2(1 - iB\hat{k}_\beta^2\zeta/2)\hat{r}\hat{r}'\cos(\hat{k}_\beta\zeta)}{\sin^2(\hat{k}_\beta\zeta)}\right]$$

Analytical techniques are used to calculate radiation fields in the linear mode of operation, and time-dependent numerical simulation codes are used in the general case.
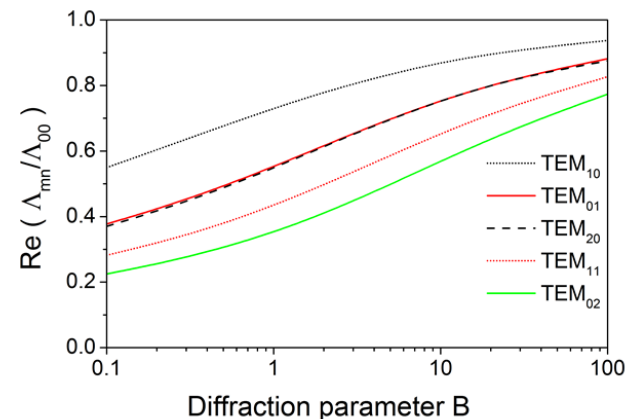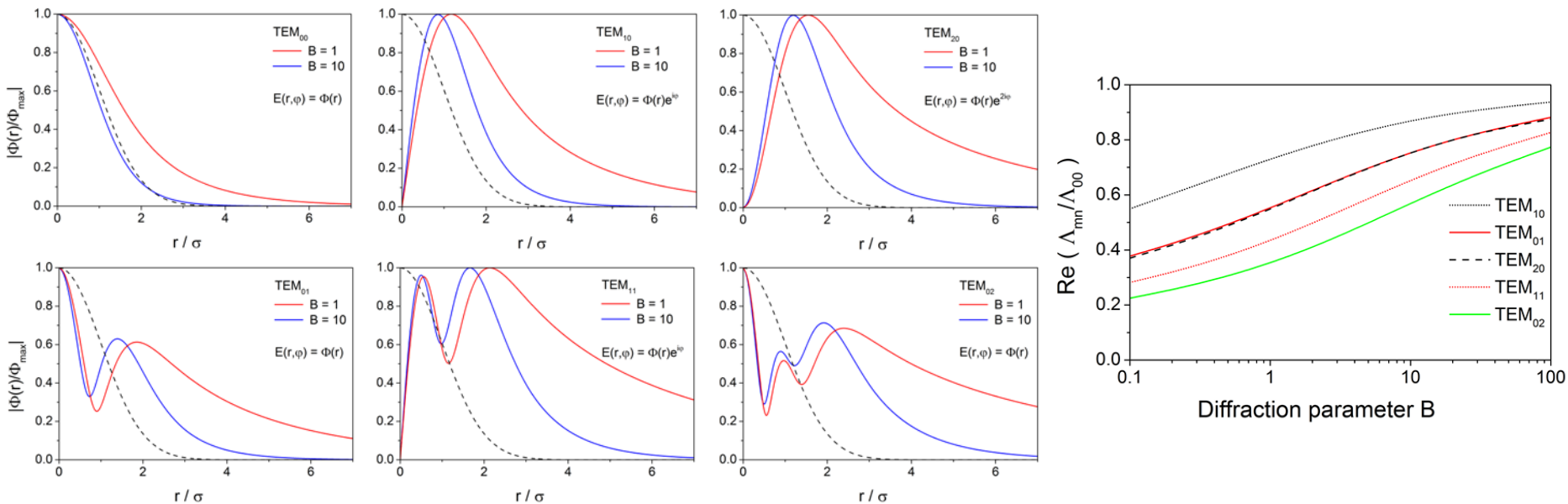
- Operation of the FEL amplifier is described by the diffraction parameter B, the energy spread parameter $\hat{\Lambda}_T^2$, and the betatron motion parameter $\hat{k}_\beta$:

$$B = 2\Gamma\sigma^2\omega/c\,, \qquad \hat{k}_\beta = 1/(\beta\Gamma)\,, \qquad \hat{\Lambda}_T^2 = (\sigma_E/\mathcal{E})^2/\rho^2\,,$$

with the gain parameter $\Gamma = 4\pi\rho/\lambda_w$.

- An effect of the mode degeneration takes place for large values of the diffraction parameter B (wide electron beam):

$$\Lambda_{mn}/\Gamma \simeq \frac{\sqrt{3}+\mathrm{i}}{2B^{1/3}} - \frac{(1+\mathrm{i}\sqrt{3})(1+n+2m)}{3\sqrt{2}B^{2/3}}$$

- The strongest higher order spatial modes are azimuthally nonsymmetric modes TEM_{10} and TEM_{20}.
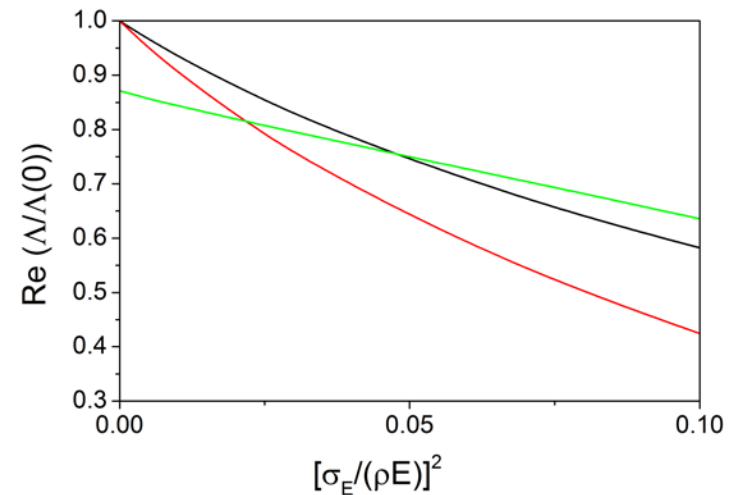
Self-reproducing FEL radiation modes
Mode degeneration

- Operation of the FEL amplifier is described by the diffraction parameter B, the energy spread parameter $\hat{\Lambda}_T^2$, and the betatron motion parameter $\hat{k}_\beta$:

$$B = 2\Gamma\sigma^2\omega/c \,, \qquad \hat{k}_\beta = 1/(\beta\Gamma) \,, \qquad \hat{\Lambda}_T^2 = (\sigma_E/\mathcal{E})^2/\rho^2 \,,$$

with the gain parameter $\Gamma = 4\pi\rho/\lambda_w$.

- Increase of emittance and the energy spread results in suppression of the mode degeneration effect for the price of the gain reduction of the fundamental mode TEM_{00} mode.
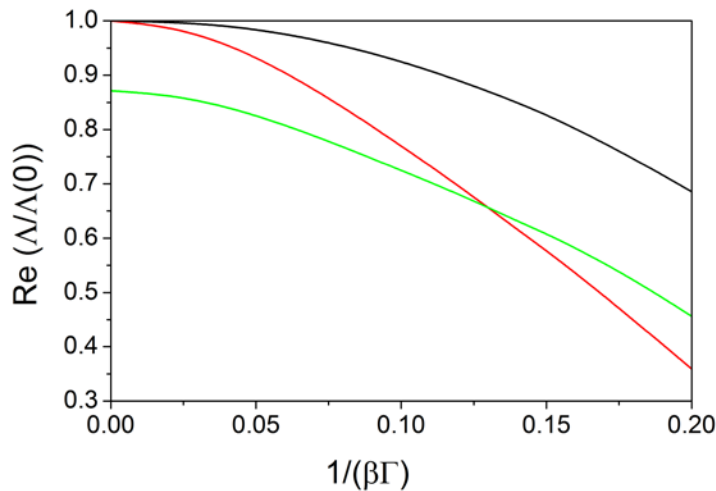
Suppression of the mode degeneration for B = 10

Self-reproducing FEL radiation modes
Mode degeneration

- In the linear high-gain limit the radiation emitted by the electron beam in the undulator can be represented as a set of modes:

$$E_{\mathrm{x}} + iE_{\mathrm{y}} = \int d\omega \exp[i\omega(z/c - t)] \times \sum_{n,k} A_{nk}(\omega, z)\Phi_{nk}(r, \omega) \exp[\Lambda_{nk}(\omega)z + in\phi] .$$

- A large number of transverse radiation modes are excited when the electron beam enters the undulator. These radiation modes have different gain. As undulator length progresses, the fundamental Φ_{00} mode predominate more and more over higher spatial modes.

- Parameter space of long wavelength x-ray FELs corresponds to the case of diffraction limited electron beams. Radiation modes in this case are well separated in the gain, and it is possible to obtain a high degree of transverse coherence in the saturation point.

- Parameter space of short wavelength XFELs correspond to the case of the wide electron beam, and the mode degeneration effect prevents suppression of higher spatial modes. The consequences are:

  - Degradation of transverse coherence;
  - Complicated and essentially non-gaussian field distributions across the slices of the radiation pulse which happens due to interference of many statistically independent spatial modes;
  - Poor pointing stability.

- These effects stems from fundamental origin - start-up of the amplification process from the shot noise in the electron beam.
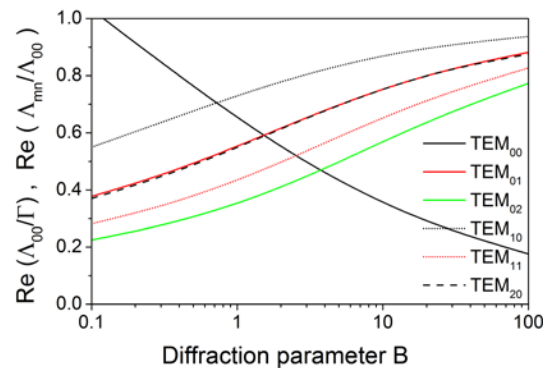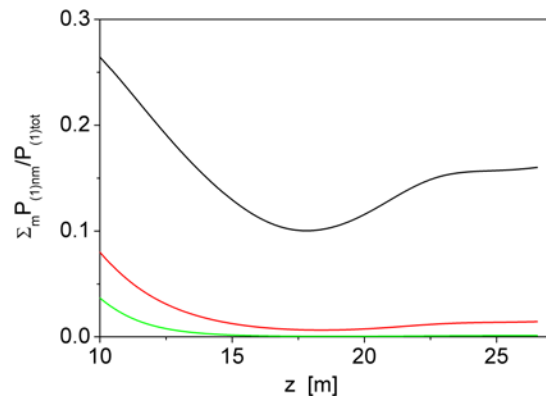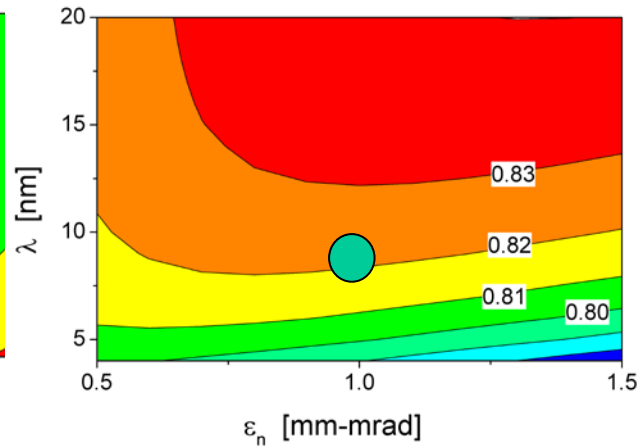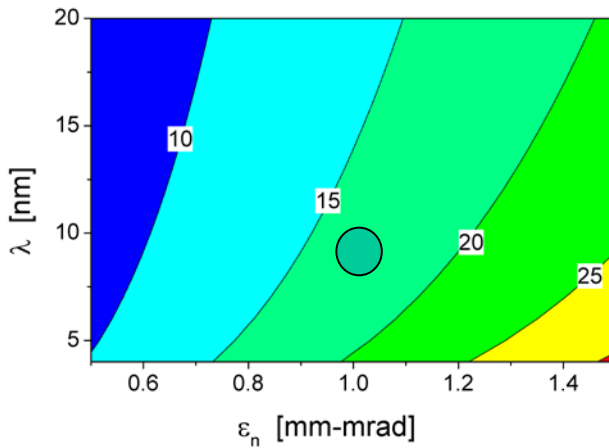
FLASH: experiment
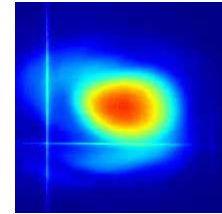
FLASH: FAST simulations

Parameter space of FLASH:

Large values of diffraction parameter (B = 10 - 25) and "cold" electron beam.

Mode degeneration effect is strong (gain of TEM_{10} mode is 0.8 – 0.83 of the fundamental TEM_{00}).

Contribution of the first azimuthal mode to the total power is 10 to 15%.

Result: unstable shape and pointing of the photon pulse.

- Typical procedure of optimization of short wavelength SASE FEL consists in optimization for the maximum gain of the fundamental (TEM_{00}) beam radiation mode. This case is referred as optimized x-ray FEL.

- Gain and optimum beta function in the case of small energy spread:

$$L_\mathrm{g} \simeq 1.67 \left(\frac{I_A}{I}\right)^{1/2} \frac{(\epsilon_n \lambda_\mathrm{w})^{5/6}}{\lambda^{2/3}} \frac{(1+K^2)^{1/3}}{K A_{JJ}} \, , \qquad \beta_\mathrm{opt} \simeq 11.2 \left(\frac{I_A}{I}\right)^{1/2} \frac{\epsilon_n^{3/2} \lambda_\mathrm{w}^{1/2}}{\lambda K A_{JJ}} \, .$$

- Application of similarity techniques to the FEL equations gives elegant result: characteristics of SASE FEL written down in the normalized form are functions of two parameters, ratio of geomtrical emittance to the wavelength, and the number of electrons in the volume of coherence:

$$\hat{\epsilon} = 2\pi\epsilon/\lambda \, , \qquad N_\mathrm{c} = I L_\mathrm{g} \lambda / (e \lambda_\mathrm{w} c) \, .$$

- Dependence of the FEL characterestics on N_c is very slow, in fact, logarithmic. Approximately, with logarithmic accuracy they depend only on $\hat{\epsilon}$.

- In fact, the diffraction parameter B and the betatron oscillation parameter k_β are:

$$B \simeq 13 \times \hat{\epsilon}^{5/2} \, , \qquad k_\beta \simeq 0.154/\hat{\epsilon}^{3/2}$$

Optimized XFEL at saturation

Saturation length:

$$\hat{L}_{sat} = \Gamma L_{sat} \simeq 2.5 \times \hat{\epsilon}^{5/6} \times \ln N_c \; ,$$

FEL efficiency:

$$\hat{\eta} = P/(\bar{\rho}P_b) \simeq 0.17/\hat{\epsilon} \; ,$$

Coherence time and rms spectrum width:

$$\hat{\tau}_c = \bar{\rho}\omega\tau_c \simeq 1.16 \times \sqrt{\ln N_c} \times \hat{\epsilon}^{5/6} \; , \quad \sigma_\omega \simeq \sqrt{\pi}/\tau_c \; .$$

Degree of transverse coherence:

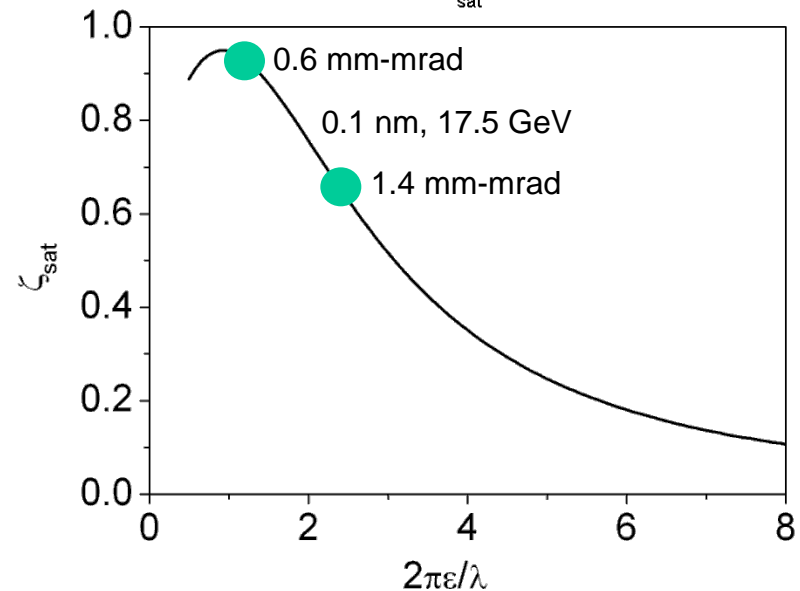$$\zeta_{sat} \simeq \frac{1.1\hat{\epsilon}^{1/4}}{1 + 0.15\hat{\epsilon}^{9/4}} \; ,$$
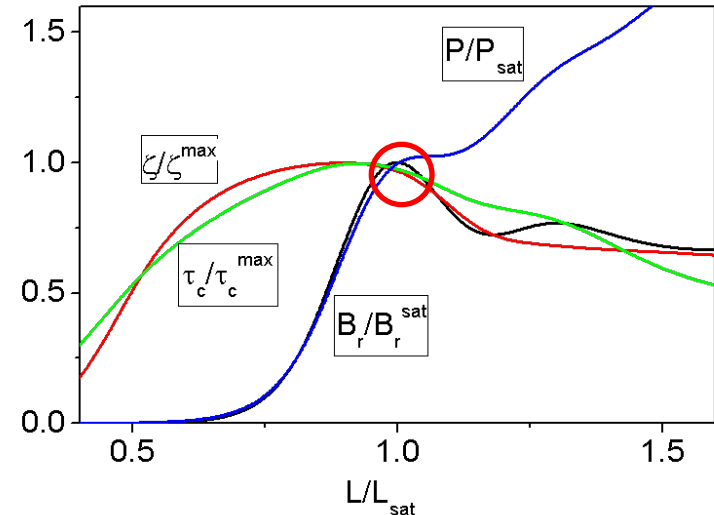
Degeneracy parameter:

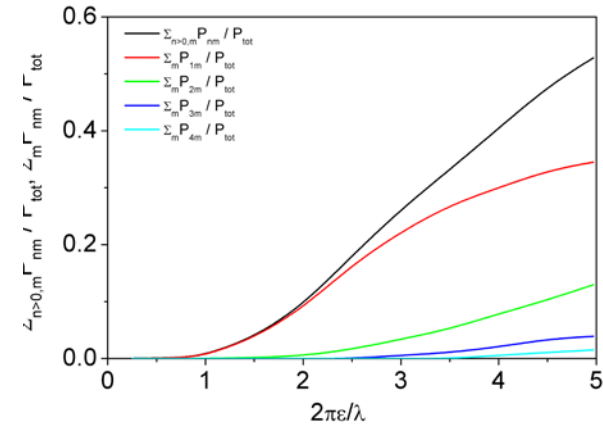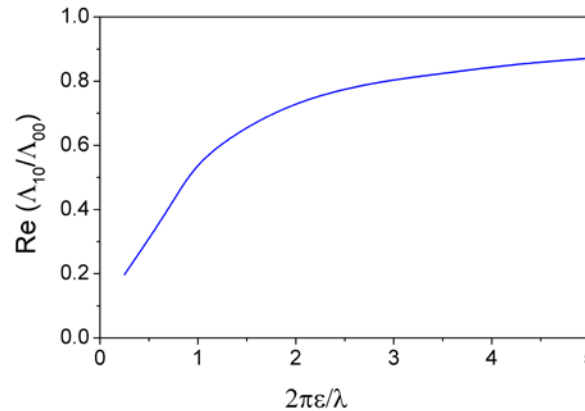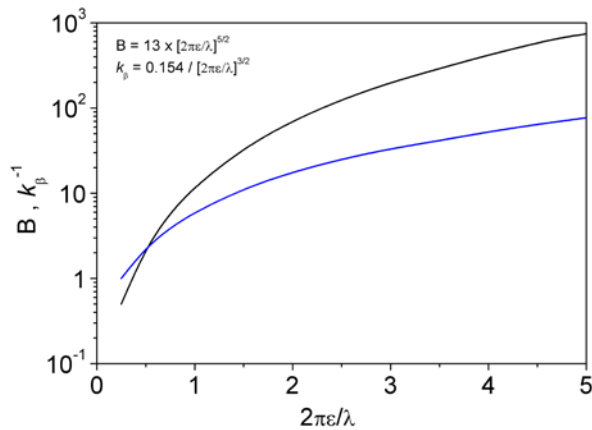$$\hat{\delta} = \hat{\eta}\zeta\hat{\tau}_c$$

Brilliance:

$$B_r = \frac{\omega d\dot{N}_{ph}}{d\omega}\frac{\zeta}{\left(\frac{\lambda}{2}\right)^2} = \frac{4\sqrt{2}c}{\lambda^3}\frac{P_b}{\hbar\omega^2}\hat{\delta} \; .$$

Normalizing parameters:

$$\Gamma = \left[\frac{I}{I_A}\frac{8\pi^2 K^2 A_{JJ}^2}{\lambda\lambda_w\gamma^3}\right]^{1/2} \; , \quad \bar{\rho} = \frac{\lambda_w\Gamma}{4\pi} \; .$$

Optimized x-ray FEL

- Features of optimized x-ray FEL for parameter space $2\pi\epsilon/\lambda > 1$:

- Large values of the diffraction parameter.

- Mode degeneration effect takes place.

- Significant contribution of higher azimuthal radiation modes.

- Poor spatial coherence.

- Complicated and essentially non-gaussian field distributions across slices of the radiation pulse.

- Poor pointing stability of the radiation.
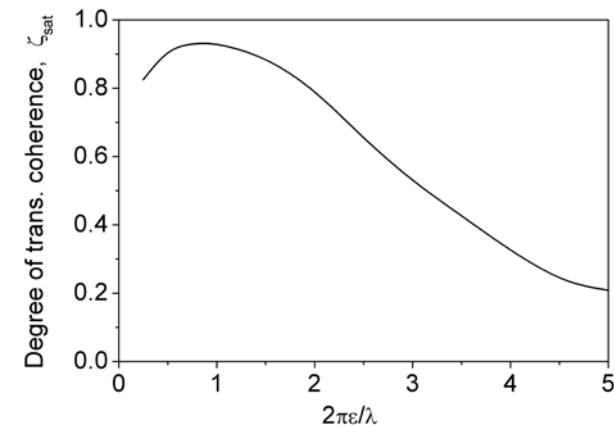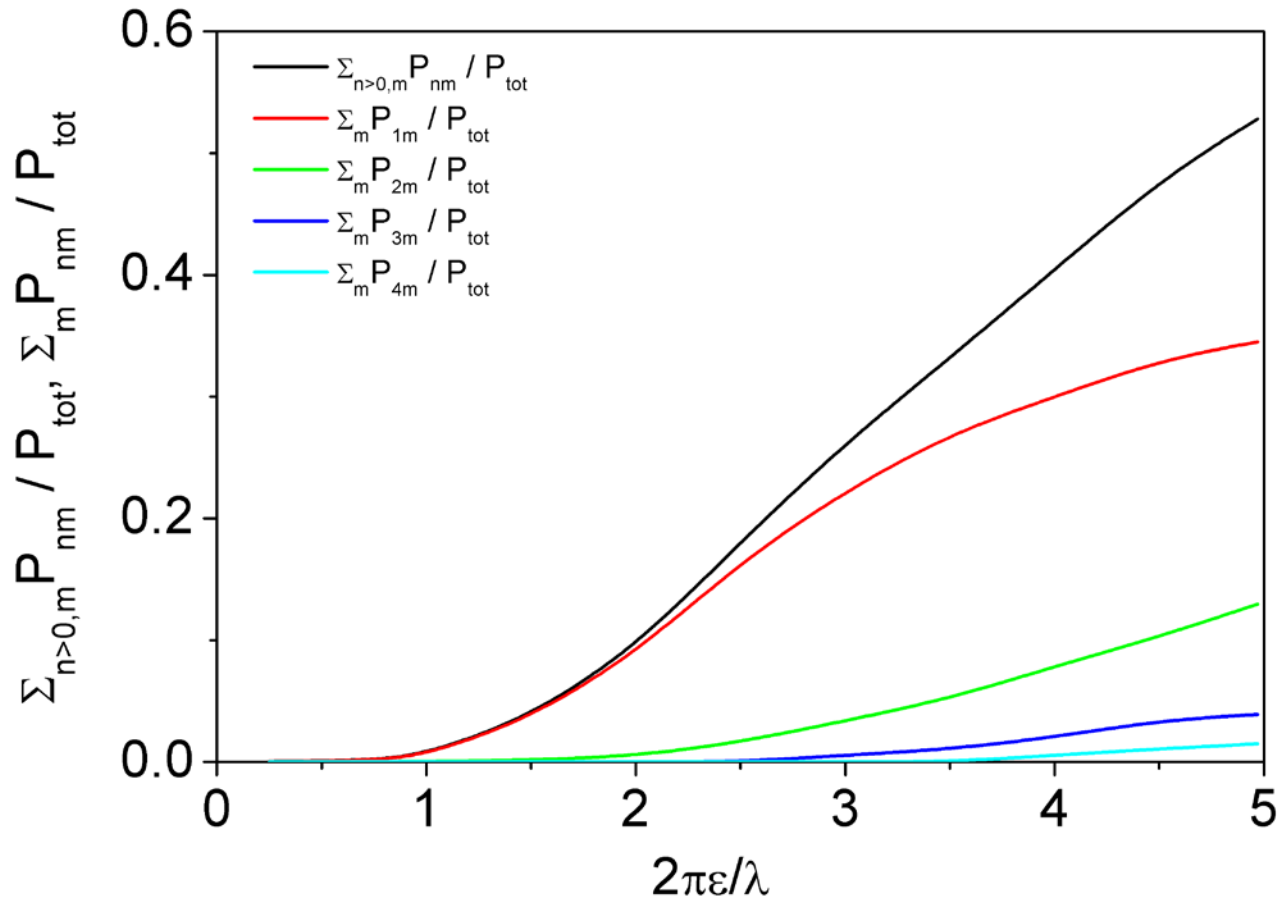
$$E_x + iE_y = \int d\omega \exp[i\omega(z/c - t)] \times \sum_{n,k} A_{nk}(\omega, z)\Phi_{nk}(r, \omega) \exp[\Lambda_{nk}(\omega)z + in\phi]$$

Contribution to the total saturation power of the radiation modes with higher azimuthal indexes 1, 2, 3, 4… grows with the emittance.

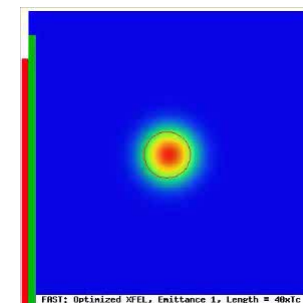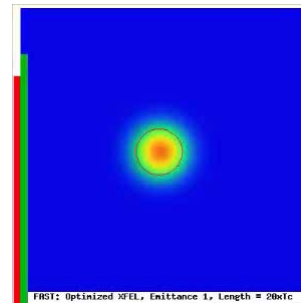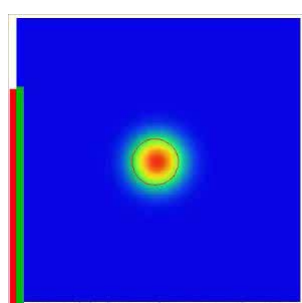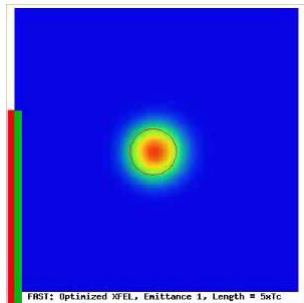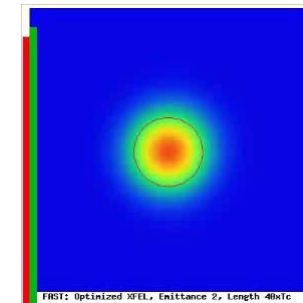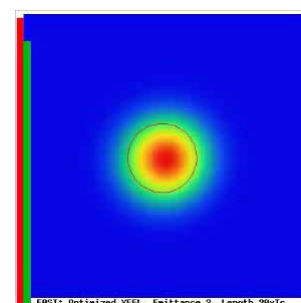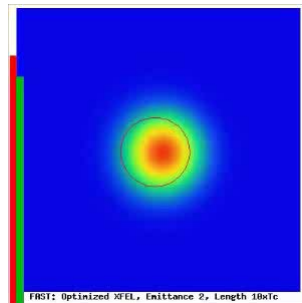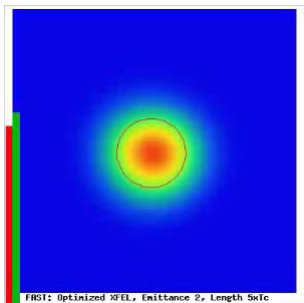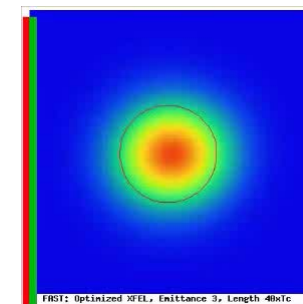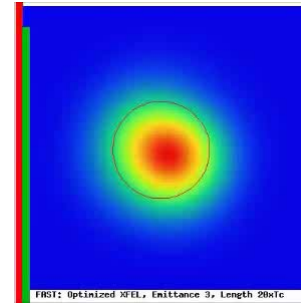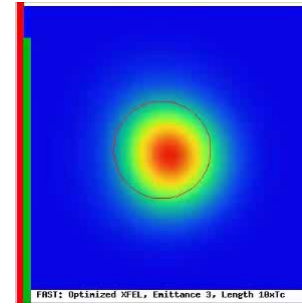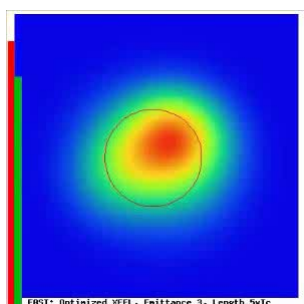- Single shot photon beam images for pulse durations $T = M \times \tau_c = 5, 10, 20,$ and 40, and emittances $2\pi\epsilon/\lambda = 1, 2,$ and 3.

Optimized x-ray FEL

Single shot images in the far zone for $2\pi\epsilon/\lambda = 1, 2, 3, 4$ (top row). Plots of σ_θ, Δ_θ, $p(\theta/\sigma_\theta)$, and $F(\theta/\sigma_\theta)$ (bottom row).
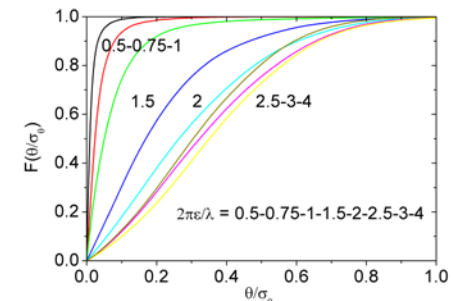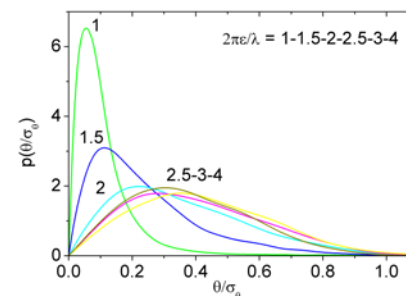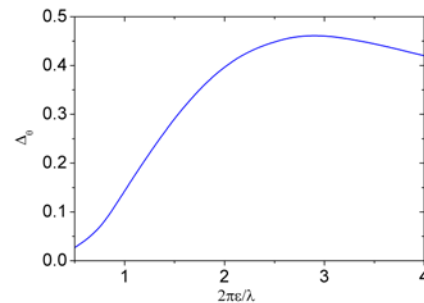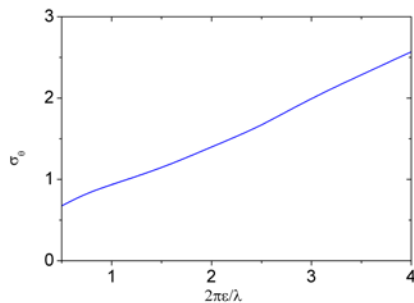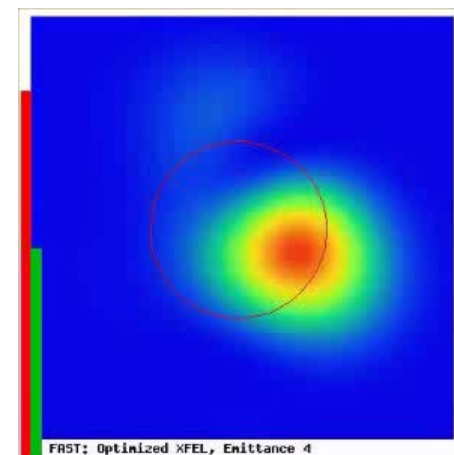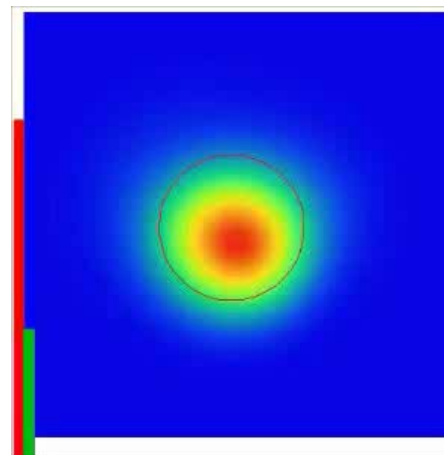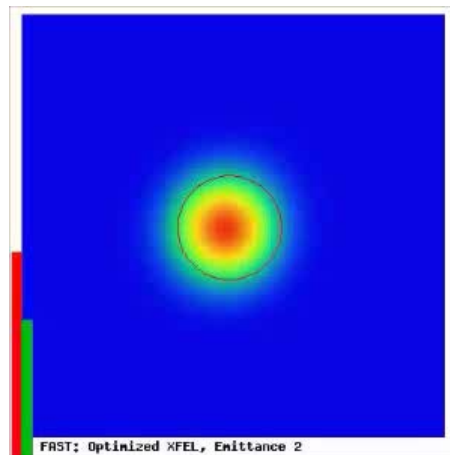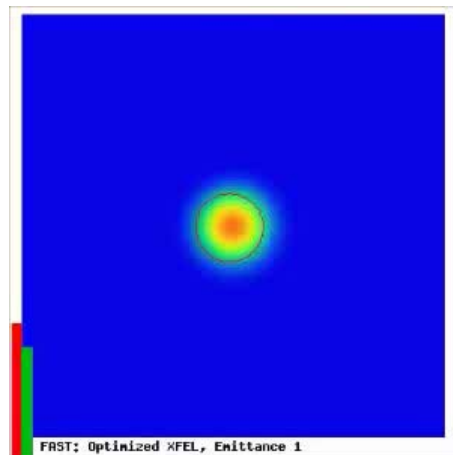
- Single shot images in the far zone for $2\pi\epsilon/\lambda = 1, 2, 3, 4$.

- Averaged rms size of the photon beam σ_θ in units of $\lambda/(2^{3/2}\pi\sigma)$.

- rms deviation of the photon beam center of gravity Δ_θ in units of averaged rms size of the photon beam.

- Probability distribution of the photon beam center of gravity, $P(\theta/\sigma_\theta)$.

- Cumulative probability distribution, $F(\theta/\sigma_\theta)$.

	LCLS	SACLA	EXFEL	SWISS FEL	PAL XFEL
Energy [GeV]	13.6	8.0	17.5	5.8	10
Wavelength [A]	1.5	0.6	0.5	0.7	0.6
ϵ_n [mm-rad]	0.4	0.4	0.4	0.4	0.4
$\hat{\epsilon} = 2\pi\epsilon/\lambda$	1	2.7	1.5	3.4	2.1

M.V. Yurkov, Coherence properties of the radiation from SASE FEL, CERN Accelerator School on FELs and ERLs, 31 May – 10 June, 2016

- Practical example: European XFEL, SASE3, radiation wavelength 1.6 nm.

- General feature of tapered regime is that both, spatial and temporal coherence degrade in the nonlinear regime, but a bit slowly than for untapered case.

- Peak brilliance grows due to the growth of the radiation power, and reaches maximum value in the middle of tapered section. Benefit in the peak brilliance is about factor of 3 with respect to untapered case.

- Spatial corellations and degree of transverse coherence:

$$\gamma_1(\vec{r}_\perp, \vec{r}\prime_\perp, z, t) = \frac{\langle \tilde{E}(\vec{r}_\perp, z, t)\tilde{E}^*(\vec{r}\prime_\perp, z, t)\rangle}{\left[\langle|\tilde{E}(\vec{r}_\perp, z, t)|^2\rangle\langle|\tilde{E}(\vec{r}\prime_\perp, z, t)|^2\rangle\right]^{1/2}} ,$$

$$\zeta = \frac{\int |\gamma_1(\vec{r}_\perp, \vec{r}\prime_\perp)|^2 I(\vec{r}_\perp)I(\vec{r}\prime_\perp)\, d\vec{r}_\perp\, d\vec{r}\prime_\perp}{[\int I(\vec{r}_\perp)\, d\vec{r}_\perp]^2} ,$$

- Temporal corellations and coherence time:

$$g_1(\vec{r}, t - t') = \frac{\langle \tilde{E}(\vec{r}, t)\tilde{E}^*(\vec{r}, t')\rangle}{\left[\langle|\tilde{E}(\vec{r}, t)|^2\rangle\langle|\tilde{E}(\vec{r}, t')|^2\rangle\right]^{1/2}} , \qquad \tau_{\rm c} = \int_{-\infty}^{\infty} |g_1(\tau)|^2\, d\tau .$$

Power and brilliance
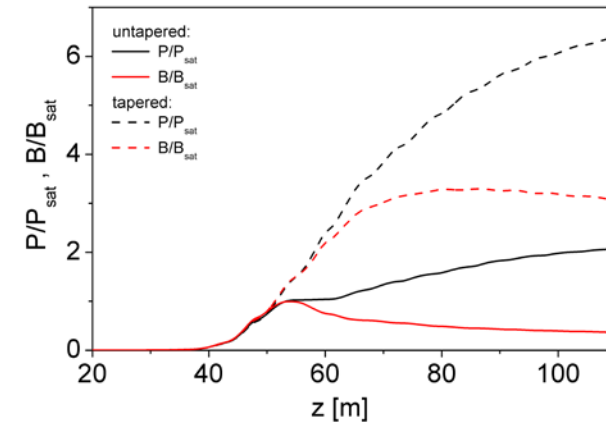
Degree of transverse coherence
Coherence time
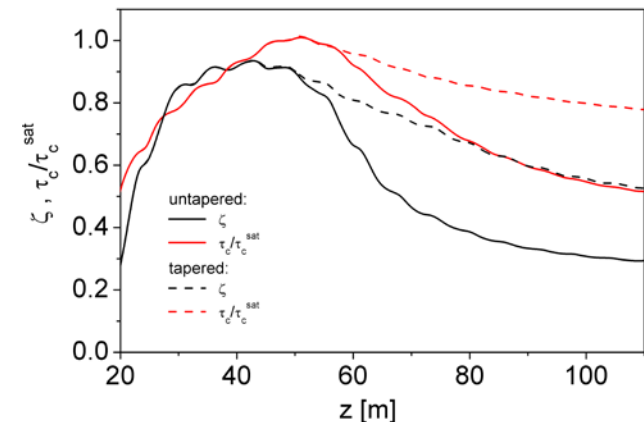
Summary on transverse coherence

- When transverse size of the electron beam exceeds diffraction limit, the mode competition effect does not provide the selection of the fundamental FEL mode, and higher order spatial modes start to contribute to the radiation power.

- The consequence of interference of statistically independent spatial modes are:
  - Degradation of transverse coherence;
  - Fluctuations of the shape and pointing stability of the photon beam (both, slice and full shot).
  - Complicated and essentially non-gaussian field distributions across the slice.

- These effects stems from fundamental origin -- start-up of the amplification process from the shot noise in the electron beam. They become pronouncing at the very early stage of the degradation of the transverse coherence due to the growing contribution of the azimuthally non-symmetric modes.

- X-ray FELs operating at short wavelengths will demonstrate degradation of the slice field patterns and the pointing stability with the increase of the parameter $2\pi\varepsilon/\lambda > 1$.
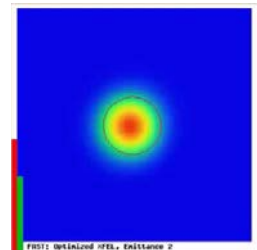
Outline

I. Start-up of the FEL process from shot noise: SASE FEL.

II. Longitudinal coherence (temporal and spectral properties). Statistics.

III. Transverse coherence.

IV. Higher harmonics.

- Radiation from SASE FEL with planar undulator contains visible contributions of odd harmonics, as well as incoherent radiation from undulator.

- Statistical properties of the odd harmonic of the radiation from SASE FEL differ significantly from those of fundamental harmonic and incoherent undulator radiation.

- An origin of this difference is that the process of generation of the harmonics in the SASE FEL is nonlinear transformation from the fundamental harmonic.

Instantaneous power

Average power
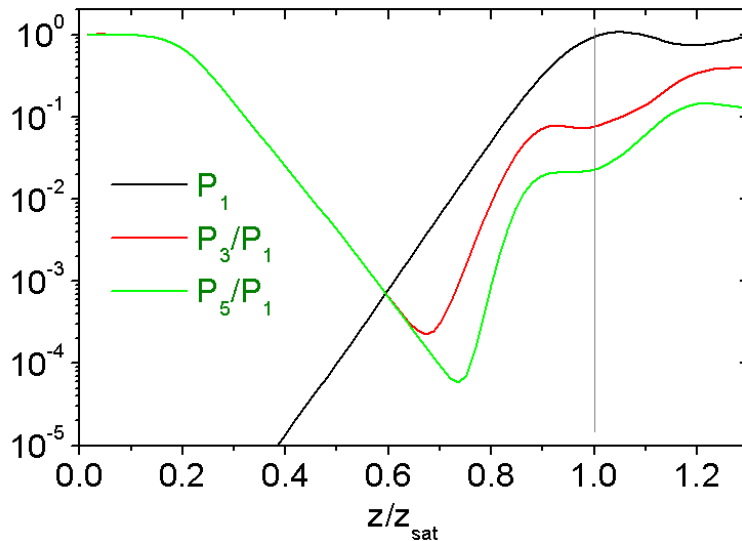
Temporal structure of the higher harmonics exhibits more spiky behavior with respect to the fundamental.
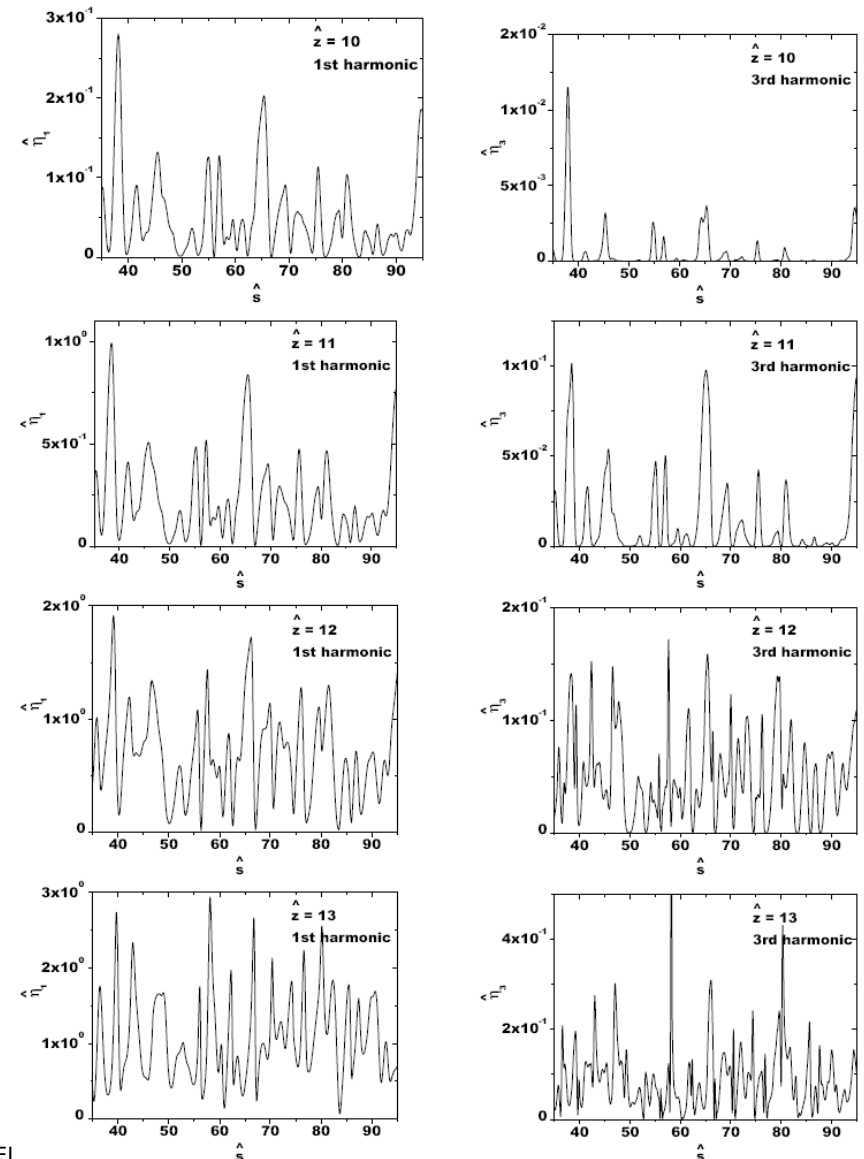
- The statistics of the high-harmonic radiation from the SASE FEL operating in the linear regime changes significantly with respect to the fundamental harmonic (e.g., with respect to Gaussian statistics).

- The probability density function of the fundamental intensity W:

$$p(W) = \langle W \rangle^{-1} \exp(-W/\langle W \rangle)$$

is subjected to a transformation $z = (W)^n$.

- The probability density function $p(z)$ is:

$$p(z) = \frac{z}{n\langle W \rangle} z^{(1-n)/n} \exp(-z^{1/n}/\langle W \rangle) .$$

- Probability distribution of the instantaneous power of higher harmonics in saturation regime is close to the negative exponential distribution.

Evolution of probability distributions for the 1st and the 3rd harmonics

M.V. Yurkov, Coherence properties of the radiation from SASE FEL, CERN Accelerator School on FEL
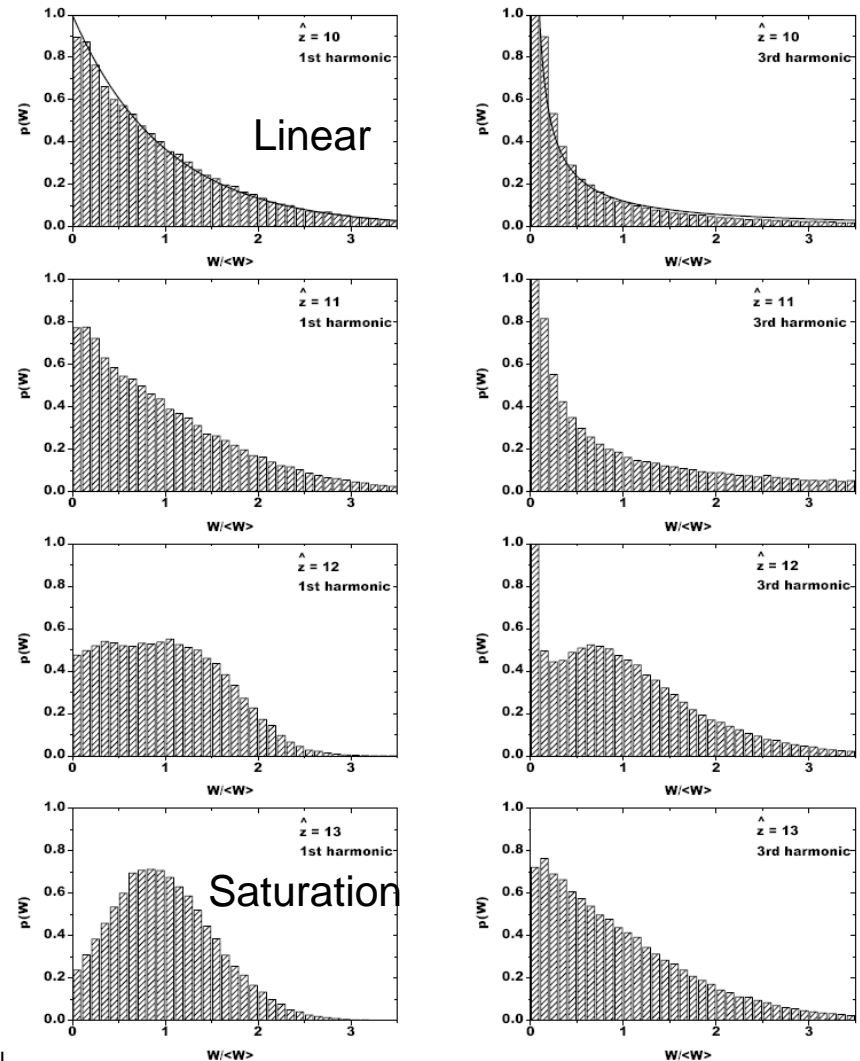
- In the saturation a universal dependency holds for the ratio of the power in the higher harmonics with respect to the fundamental one:

$$\frac{\langle W_3 \rangle}{\langle W_1 \rangle}\bigg|_{\text{sat}} = f_3(\hat{\Lambda}_T^2) \times \frac{K_3^2}{K_1^2} \ ,$$

$$\frac{\langle W_5 \rangle}{\langle W_1 \rangle}\bigg|_{\text{sat}} = f_5(\hat{\Lambda}_T^2) \times \frac{K_5^2}{K_1^2} \ .$$

$$K_h = K(-1)^{(h-1)/2}[J_{(h-1)/2}(Q) - J_{(h+1)/2}(Q)]$$

$$Q = K^2/[2(1+K^2)]$$

XFEL with planar undulator: odd harmonics
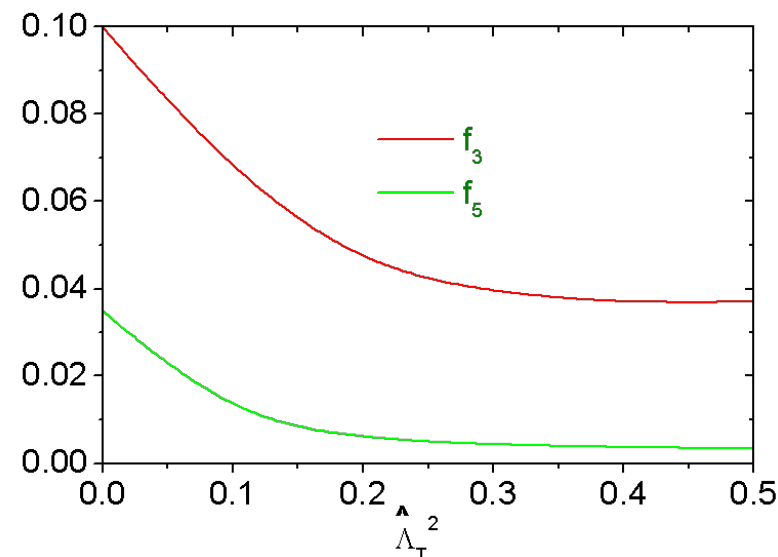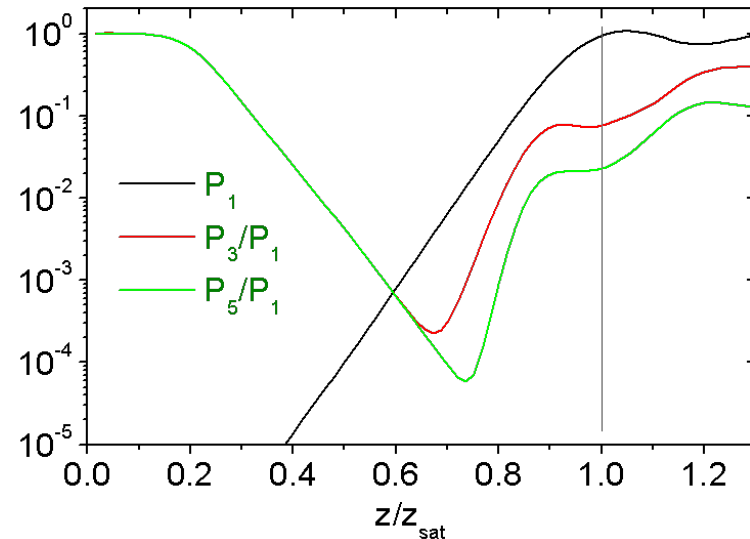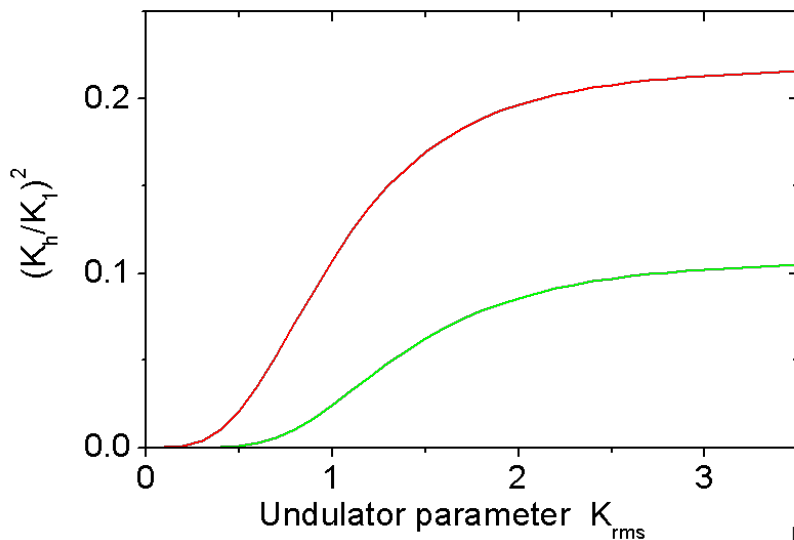
- Contributions of the higher odd harmonics to the FEL power for SASE FEL operating at saturation are universal functions of the undulator parameter K.

- Power of higher harmonics is subjected to larger fluctuations than that of the fundamental one.

- Probability distributions of the instantaneous power of higher harmonics in saturation regime is close to the negative exponential distribution.

- The coherence time in saturation falls inversely proportional to harmonic number: $\tau_c \propto 1/h$.

- Relative spectrum bandwidth remains constant with harmonic number.

Coherence time: 1st, 3rd, 5th
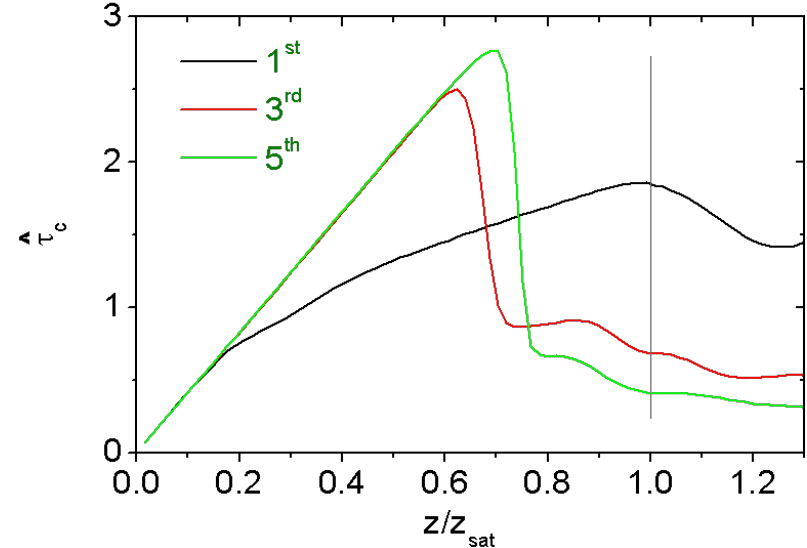
Average spectra: 1st, 3rd, 5th

$$\Delta\omega = -2\rho\omega_h \hat{C}$$

M.V. Yurkov, Coherence properties of the radiation from SASE FEL, CERN Accelerator School on FELs and ERLs, 31 May – 10 June, 2016
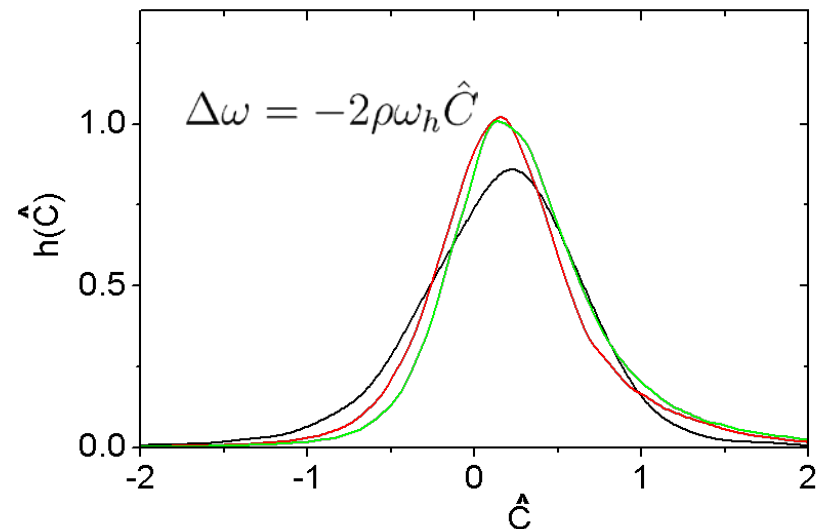
- Coherence time in the nonlinear regime falls down proportionally to the harmonic number.

- Degree of transverse coherence of higher harmonics is less than that of the fundamental.

- Contribution of higher harmonics to the total power grows in the deep nonlinear regime, and may constitute substantial amount.

- Maximum of the brilliance of the higher harmonics occurs in the deep nonlinear regime.
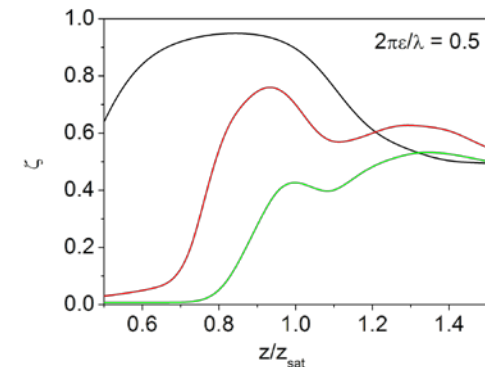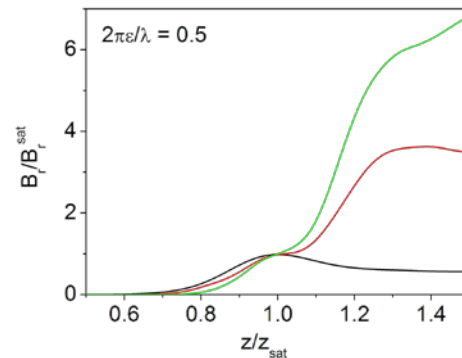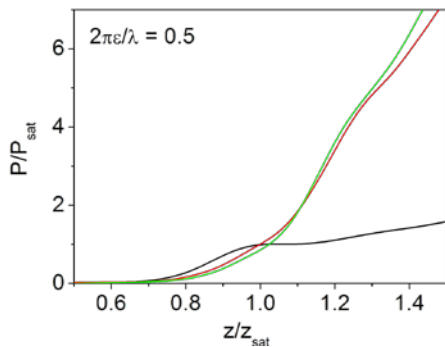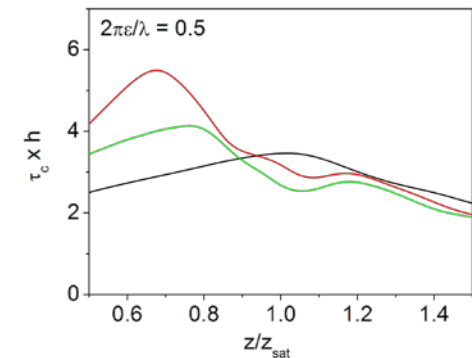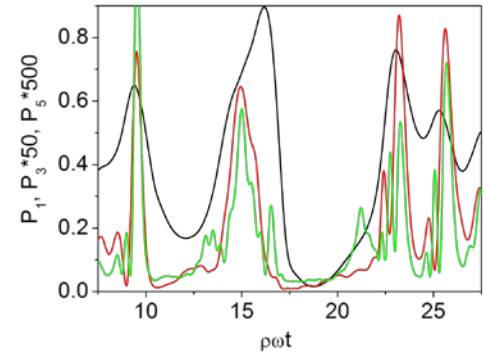
Optimized XFEL with planar undulator: odd harmonics
Diffraction effects

- Degree of transverse coherence of higher harmonics falls down with harmonic number, and significantly degrades with growth of the parameter $\hat{\epsilon} = 2\pi\epsilon/\lambda$.

- The dependencies for the ratios of the power of higher harmonics to the fundamental are universal functions of emittance parameter when we factorize them with factor A_{JJh}^2/A_{JJ1}^2.

- For large values of the undulator parameter K asymptotic values of A_{JJh}^2/A_{JJ1}^2 are equal to 0.22 and 0.11 for the 3rd and the 5th harmonic, respectively. In the range of emittance parameter from 0.25 to 2 contributions to the total power of the 3rd (5th) harmonic is between 0.3 - 1.4% (0.07 - 0.16%).

Summary
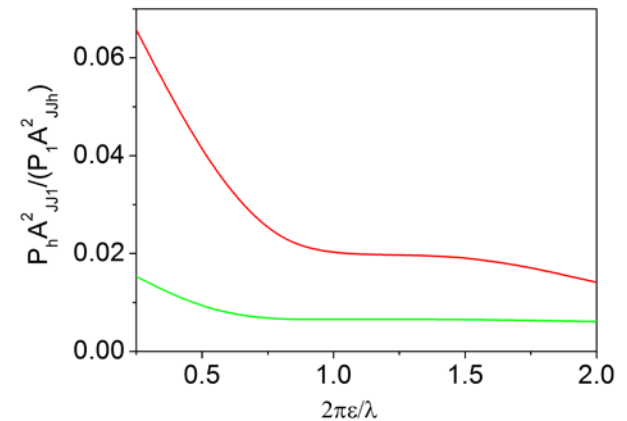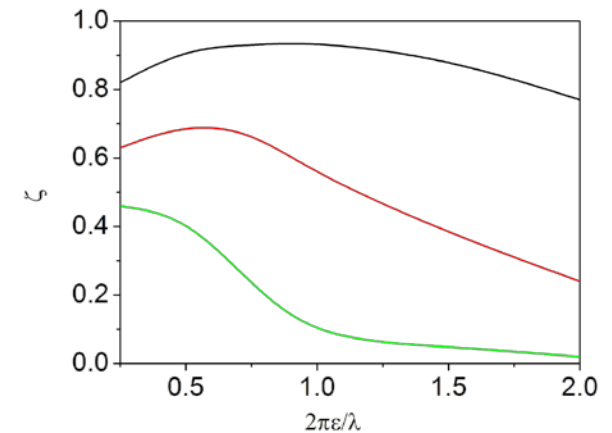
- This lecture presents an overview of the properties of the radiation from x-ray free electron lasers. Simple formulae allow one to obtain quantitative description of the SASE FEL operating in the saturation regime.

- For more details we address you to suggested further reading which highlights theoretical developments, up-to-date experimental activity at FLASH, LCLS, SACLA, and projects of XFELs to be realized soon: SWISS XFEL, PAL XFEL, and European XFEL.

Thank you for your attention!

Suggested bibliography

A. FEL theory:

1. E.L. Saldin, E.A. Schneidmiller, and M.V. Yurkov, The Physics of Free Electron Lasers (Springer-Verlag, Berlin, 1999).
2. E.L. Saldin, E.A. Schneidmiller and M.V. Yurkov, A simple method for the determination of the structure of ultrashort relativistic electron bunches, Nucl. Instrum. and Methods A539(2005)217.
3. E.L. Saldin, E.A. Schneidmiller, and M.V. Yurkov, Statistical properties of radiation from VUV and X-ray free electron lasers, Optics Communications 148(1998)383.
4. E.L. Saldin, E.A. Schneidmiller, and M.V. Yurkov, Diffraction effects in the self-amplified spontaneous emission FEL, Optics Communications 186(2000)185.
5. E.L. Saldin, E.A. Schneidmiller, and M.V. Yurkov, Statistical properties of radiation from SASE FEL driven by short electron bunches, Nucl. Instrum. and Methods A507(2003)101.
6. E.L. Saldin, E.A. Schneidmiller, and M.V. Yurkov, Coherence properties of the radiation from X-ray free electron laser, Optics Communications, 281(2008)1179.
7. E.L. Saldin, E.A. Schneidmiller, and M.V. Yurkov, Output power and degree of transverse coherence of X-ray free electron lasers, Optics Communications, 281(2008)4727.
8. E.L. Saldin, E.A. Schneidmiller, and M.V. Yurkov, Statistical and coherence properties of radiation from x-ray free-electron lasers, New J. Phys. 12 (2010) 035010.
9. G. Geloni et al., Coherence properties of the European XFEL, New J. Phys. 12 (2010) 035021.
10. E.A. Schneidmiller and M.V. Yurkov, Statistical properties of the radiation from SASE FEL operating in a post-saturation regime with and without undulator tapering,, Journal of Modern Optics, Special Issue Short Wavelength Free Electron Lasers and their Interactions with Matter 2015, DOI:10.1080/09500340.2015.1035349.
11. E.A. Schneidmiller and M.V. Yurkov, Coherencece properties of the radiation from FLASH, Journal of Modern Optics, Special Issue Short Wavelength Free Electron Lasers and their Interactions with Matter 2015, DOI:10.1080/09500340.2015.1066456.
12. E.A. Schneidmiller and M.V. Yurkov, Fundamental Limitations of the SASE FEL Photon Beam Pointing Stability, Proc. FEL2015, TUP021.
13. E.A. Schneidmiller and M.V. Yurkov, Transverse Coherence and Fundamental Limitatiton on the Pointing Stability of X-ray FELs , Proc. IPAC2016, MOPOW011.
14. E.L. Saldin, E.A. Schneidmiller, and M.V. Yurkov, Properties of the third harmonic of the radiation from self-amplified spontaneous emission free electron laser, Phys. Rev. ST Accel. Beams 9(2006)030702.
15. P. Schmüser, M. Dohlus, J. Rossbach, C. Behrens, Free-Electron Lasers in the Ultraviolet and X-Ray Regime (Springer-Verlag, Berlin, 2014).
16. Z. Huang and K.-J. Kim, Review of x-ray free electron laser theory, Phys. Rev. ST Accel. Beams 10(2007)034801.

B. Statistical optics

1. J. Goodman, Statistical Optics, (John Wiley and Sons, New York, 1985).

C. Experimental activity at DESY (TTF FEL, FLASH):

1. V. Ayvazyan et al., Generation of GW radiation pulses from a VUV free-electron laser operating in the femtosecond regime, Phys. Rev. Lett. 88(2002)10482.
2. V. Ayvazyan et al., First operation of a free-electron laser generating GW power radiation at 32 nm wavelength, The European Physical Journal D 37(2006)297.
3. W. Ackermann et al., Operation of a free electron laser from the extreme ultraviolet to the water window, Nature Photonics, 1 (2007)336.
4. M. Dohlus et al., Start-to-end simulations of SASE FEL at the TESLA Test Facility, phase 1, Nucl. Instrum. and Methods A530(2004)217.
5. V. Ayvazyan et al., Study of the statistical properties of the radiation from a VUV SASE FEL operating in the femtosecond regime, Nucl. Instrum. and Methods A507(2003)368.
6. R. Ischebeck et al., Study of the transverse coherence at the TTF free electron laser, Nucl. Instrum. and Methods A507(2003)175.
7. E.L. Saldin, E.A. Schneidmiller, and M.V. Yurkov, Statistical properties of the radiation from VUV FEL at DESY operating at 30 nm wavelength in the femtosecond regime, Nucl. Instrum. and Methods A562(2006)472.
8. E.A. Schneidmiller, and M.V. Yurkov, Application of Statistical Methods for Measurements of the Coherence Properties of the Radiation from SASE FEL, Proc. IPAC2016, MOPOW013.
9. C. Behrens et al., Constraints on photon pulse duration from longitudinal electron beam diagnostics at a soft x-ray free-electron laser, Phys. Rev. ST Accel. Beams 15 (2012) 030707.
10. S. Duesterer et al., Development of experimental techniques for the characterization of ultrashort photon pulses of extreme ultraviolet free-electron lasers, Phys. Rev. ST Accel. Beams 17 (2014) 120702.
11. P. Schmüser, M. Dohlus, J. Rossbach, C. Behrens, Free-Electron Lasers in the Ultraviolet and X-Ray Regime (Springer-Verlag, Berlin, 2014).

D. Experimental activity at XFELs:

1. P. Emma et al., First lasing and operation of an angstrom-wavelength free-electron laser, Nature Photonics, 4(2010)641.
2. A.A. Lutman et al, Polarization control in an X-ray free-electron laser, Nature Photonics, Published online 09 May 2016, 1038/nphoton.2016.79.
3. T. Ishikawa et al., A compact X-ray free-electron laser emitting in the sub-ångström region, Nature Photonics, 6(2012)540.

E. XFEL projects :

1. LCLS WEB page: https://portal.slac.stanford.edu/sites/lcls_public/
2. M. Altarelli et al. (Eds.), XFEL: The European X-Ray Free-Electron Laser. Technical Design Report, Preprint DESY 2006-097, DESY, Hamburg, 2006 (see also http://xfel.desy.de).
3. J. Arthur et al., Linac Coherent Light Source (LCLS). Conceptual Design Report, SLAC- R593, Stanford, 2002 (see also http://www-ssrl.slac.stanford.edu/lcls/cdr).
4. T. Tanaka and T. Shintake (Eds.), SCSS X-FEL Conceptual Design Report. Riken Harima Institute, Hyogo, Japan, May 2005 (see also http://xfel.riken.jp/eng/).
5. SWISSFEL WEB page: https://www.psi.ch/swissfel/
6. PAL-XFEL: http://pal.postech.ac.kr/paleng/